

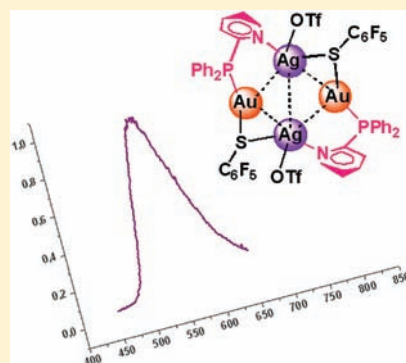
# Unprecedented Luminescent Heteropolynuclear Aggregates with Gold Thiolates as Building Blocks

Olga Crespo, M. Concepción Gimeno,\* Antonio Laguna, Fernando J. Lahoz, and Carmen Larraz

Departamento de Química Inorgánica, Instituto de Síntesis Química y Catálisis Homogénea (ISQCH), Universidad de Zaragoza-CSIC, E-50009 Zaragoza, Spain

**S** Supporting Information

**ABSTRACT:** The reaction of  $[\text{AuCl}(\text{P-N})]$ , in which P-N represents a heterofunctional phosphine ligand, with pentafluorothiophenol,  $\text{HSC}_6\text{F}_5$ , gives the thiolate gold derivatives  $[\text{Au}(\text{SC}_6\text{F}_5)(\text{P-N})]$  (P-N =  $\text{PPh}_2\text{py}$  (1),  $\text{PPh}_2\text{CH}_2\text{CH}_2\text{py}$  (2), or  $\text{PPhpy}_2$  (3)). Complex  $[\text{Au}(\text{SC}_6\text{F}_5)(\text{PPh}_2\text{py})]$  (1) reacts with  $[\text{Au}(\text{OTf})(\text{PPh}_2\text{py})]$  in a 1:1 or 1:2 molar ratio to afford the di- or trinuclear species  $[\text{Au}_2(\mu\text{-SC}_6\text{F}_5)(\text{PPh}_2\text{py})_2]\text{OTf}$  (4) and  $[\text{Au}_3(\mu_3\text{-SC}_6\text{F}_5)(\text{PPh}_2\text{py})_3](\text{OTf})_2$  (5), with the thiolate acting as a doubly or triply bridging ligand. The reactivity of the mononuclear compounds  $[\text{Au}(\text{SC}_6\text{F}_5)(\text{P-N})]$  toward silver or copper salts in different ratios has been investigated. Thus, the treatment of  $[\text{Au}(\text{SC}_6\text{F}_5)(\text{P-N})]$  with  $\text{Ag}(\text{OTf})$  or  $[\text{Cu}(\text{NCMe})_4]\text{PF}_6$  in a 1:1 molar ratio gives complexes of stoichiometry  $[\text{AuAg}(\text{OTf})(\mu\text{-SC}_6\text{F}_5)(\text{P-N})]$  (P-N =  $\text{PPh}_2\text{py}$  (6),  $\text{PPh}_2\text{CH}_2\text{CH}_2\text{py}$  (7), or  $\text{PPhpy}_2$  (8)) or  $[\text{AuCu}(\mu\text{-SC}_6\text{F}_5)(\text{P-N})(\text{NCMe})]\text{PF}_6$  (P-N =  $\text{PPh}_2\text{py}$  (9),  $\text{PPh}_2\text{CH}_2\text{CH}_2\text{py}$  (10), or  $\text{PPhpy}_2$  (11)). These complexes crystallize as dimers and display different coordination modes of the silver or copper center, depending on the present functionalized phosphine ligand. The treatment of  $[\text{Au}(\text{SC}_6\text{F}_5)(\text{PPh}_2\text{py})]$  with silver and copper compounds in other molar ratios has been carried out. In a 2:1 ratio, the complexes  $[\text{Au}_2\text{M}(\mu\text{-SC}_6\text{F}_5)_2(\mu\text{-PPh}_2\text{py})_2]\text{X}$  (M = Ag, X =  $\text{OTf}$  (12); M = Cu, X =  $\text{PF}_6$  (13)) are obtained. The same reaction in a 4:3 molar ratio affords the species  $[\text{Au}_4\text{M}_2(\mu\text{-SC}_6\text{F}_5)_3(\mu\text{-PPh}_2\text{py})_4]\text{X}_3$  (M = Ag, X =  $\text{OTf}$  (14); M = Cu, X =  $\text{PF}_6$  (15)). The crystal structures of some of these complexes reveal different interactions among the metallic  $d^{10}$  centers. The complexes display dual emission. The band at higher energy has been attributed to intraligand (IL) transitions, and the one at lower energy has been assigned to a ligand to metal (LM) charge transfer process. The latter emission is modulated by the heterometal (silver or copper).



## INTRODUCTION

The chemistry of polynuclear  $d^{10}$  metal complexes, and group 11 in particular, has attracted a great deal of attention in the past few years because of the special characteristics they show, such as their structure and their photoluminescent behavior.<sup>1</sup> These two factors are often affected by the presence of metallic  $d^{10} \cdots d^{10}$  interactions, particularly in the case of gold(I)  $\cdots$  gold(I) interactions. Aurophilic interactions are similar in strength to hydrogen bonds and are attributable to correlation and relativistic effects.<sup>2</sup> Polynuclear gold(I) derivatives generally possess intense, long-lived luminescence in the solid state with emission energies spanning the visible spectrum. Different excited-state assignments have been made for these emissions, including metal-centered (MC), ligand to metal charge transfer (LMCT), and intraligand (IL), with aggregation through aurophilic interactions thought to play a key role in producing the emissive state.<sup>1,3</sup> Chalcogen ligands are well-known in gold chemistry. Many of them show interesting luminescent properties, e.g., the chalcogenolate species  $[\text{E}(\text{AuPPh}_2\text{py})_3\text{M}]^{2+}$ , which have emissions spanning the visible spectra (blue, green, and orange). The emission energy may be influenced by the chalcogen ligand<sup>4</sup> or the high nuclearity found in some gold(I) sulfide complexes with diphosphines such as  $[\text{Au}_{12}(\mu_3\text{-S})_4(\mu\text{-dppm})_6](\text{PF}_6)_4$ .<sup>5</sup> These

emissions are clearly LMCT but enhanced by the presence of metallophilic interactions. Thiolate ligands are also well established for gold, and their complexes have been known for a long time. They are important in many fields of research. They are used in medicine as antiarthritic agents and have also shown antitumoral and anti-HIV activity. In nanoscience they can act as stabilizers of metal nanoparticles and as precursors for other sources of materials.<sup>6–8</sup> Although gold thiolates of the form  $[\text{Au}(\text{SR})]_m$ ,  $[\text{Au}(\text{SR})(\text{PR}_3)]$ , or  $[\text{Au}_2(\mu\text{-SR})(\text{PR}_3)_2]^+$  are very numerous,<sup>7a</sup> triply bridging gold thiolates of the form  $[\text{Au}_3(\mu_3\text{-SR})\text{L}_3]^{2+}$ ,<sup>7b–d</sup> or heterometallic gold thiolates, are very scarcely represented.<sup>7a</sup> Recently, D-penicillamine gold complexes have been used as building blocks to form aggregates by forming S-bridged structures with copper or silver ions;<sup>9</sup> pyridine-2-thiolate gold derivatives also form a tetranuclear gold–copper species,<sup>10</sup> and pyridine-4-thiolate leads to heteronuclear complexes with copper and chromium by coordination to the nitrogen atom of the thiolate unit.<sup>11</sup> The aim of this work is to construct luminescent metal aggregates, starting from the building blocks of stoichiometry  $[\text{Au}(\text{SC}_6\text{F}_5)(\text{P-N})]$ , which have

Received: June 10, 2011

Published: August 23, 2011

**Table 1.** Selected Bond Lengths [Å] and Angles [°] for Complex 3

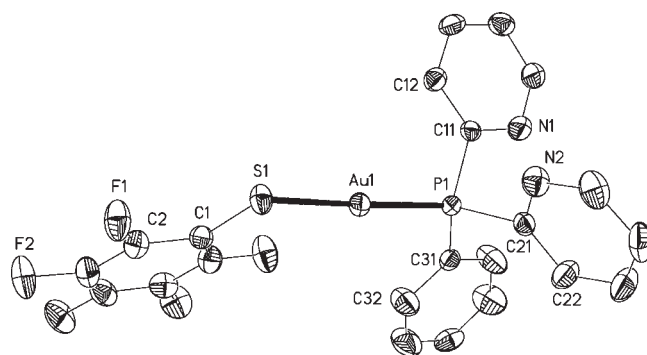
Au(1)–P(1)	2.2786(11)	P(1)–C(21)	1.845(3)
Au(1)–S(1)	2.3220(11)	N(1)–C(15)	1.355(5)
S(1)–C(1)	1.767(3)	N(1)–C(11)	1.362(5)
P(1)–C(31)	1.829(4)	N(2)–C(21)	1.344(5)
P(1)–C(11)	1.831(3)	N(2)–C(25)	1.351(5)
<hr/>			
P(1)–Au(1)–S(1)	176.90(3)	C(11)–P(1)–C(21)	101.56(15)
C(1)–S(1)–Au(1)	109.45(12)	C(15)–N(1)–C(11)	117.8(3)
C(31)–P(1)–C(11)	108.91(16)	C(21)–N(2)–C(25)	117.3(3)
C(31)–P(1)–C(21)	106.19(15)	N(2)–C(21)–P(1)	112.3(2)

functionalized tertiary phosphines such as 2-pyridil-diphenylphosphine (PPh<sub>2</sub>py), 2-pyridilethane-diphenylphosphine (PPh<sub>2</sub>CH<sub>2</sub>CH<sub>2</sub>py), or bis(2-pyridyl)phenylphosphine (PPhpy<sub>2</sub>). We have previously reported reactions of these pentafluorophenyl thiolate ligands with diphosphines and have shown that they can bridge two gold(I) or one gold(I) and one gold(III) centers.<sup>12</sup> Here the metalloligands have the nitrogen or nitrogens of the pyridine units that can be used to coordinate to other metallic centers, and the sulfur atom of the thiolate ligand can act as a multidentate coordinating site to afford sophisticated suprastructures with aurophilic or metallophilic interactions. Thus, reaction with silver or copper compounds affords heteropolynuclear aggregates, which are the first examples of simple thiolate ligands bridging different metals. These complexes exhibit luminescence properties in the solid state, and the emissive properties of these compounds have been studied in order to know the influence of the heterometal (silver or copper) in the emissions. Some of them are luminescent at both room and low temperature. At 77 K, two bands are observed for most of the complexes. The one at higher energies has been assigned to IL (monophosphine) transitions. A <sup>3</sup>LMCT (S → Au) origin is proposed for the low energy band for the metalloligands 1–3. This band is shifted to lower energies upon coordination of a heterometal. In the heterometallic complexes, the influence of the heterometal leads to different energy emissions. The nature of this band has been proposed as <sup>3</sup>LAuMCT (S → AuM).

## RESULTS AND DISCUSSION

**Synthesis of the Complexes.** The reaction of complexes [AuCl(P–N)] (P–N = PPh<sub>2</sub>py, PPh<sub>2</sub>CH<sub>2</sub>CH<sub>2</sub>py, or PPhpy<sub>2</sub>) with pentafluorothiophenol in the presence of potassium carbonate gives the thiolate gold derivatives [Au(SC<sub>6</sub>F<sub>5</sub>)(P–N)] (P–N = PPh<sub>2</sub>py (1), PPh<sub>2</sub>CH<sub>2</sub>CH<sub>2</sub>py (2), or PPhpy<sub>2</sub> (3)) in good yield. The <sup>31</sup>P{<sup>1</sup>H} NMR spectra show one resonance for the phosphorus atom at 36.61, 35.59, and 36.28 ppm. The <sup>1</sup>H NMR spectra of complexes present the resonances of the pyridine protons, although some of them are overlapped with the resonances for the phenyl protons; additionally, complex 2 shows a multiplet for the methylene protons centered at 3.16 ppm. The <sup>19</sup>F NMR spectra agree with the presence of a pentafluorophenyl moiety, and three resonances in a ratio 2:2:1 for the ortho, meta, and para fluorines appear. The liquid secondary ion mass spectra (LSIMS+) show the molecular peaks at *m/z* = 660 (1, 15%), 688 (2, 17%), and 661 (3, 63%).

The structure of complex 3 has been established by X-ray diffraction studies, and the molecule is shown in Figure 1 with a

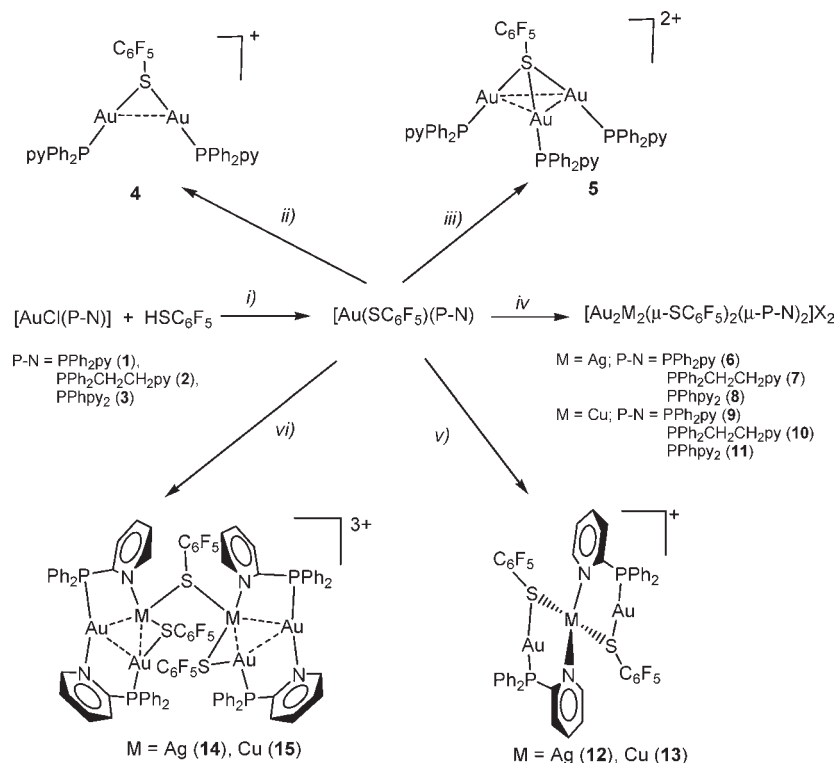


**Figure 1.** Structure of complex 3 showing the atom numbering scheme. Displacement parameter ellipsoids represent 50% probability surfaces. H atoms are omitted for clarity.

selection of bond lengths and angles in Table 1. Complex 3 crystallizes as a monomer with no short gold···gold interactions. The gold center is linearly coordinated to the thiolate and the phosphine ligand with the angle P–Au–S of 176.90(3)°. The Au–S and Au–P bond distances of 2.3220(11) and 2.2786(11) Å, respectively, are characteristic of this type of complex as, for example, the pentafluorophenyl thiolate triphenylphosphine gold complex, [Au(SC<sub>6</sub>F<sub>5</sub>)(PPh<sub>3</sub>)].<sup>13</sup>

In these thiolate gold derivatives, the sulfur atom still has two electron lone pairs and, consequently, can further coordinate additional gold fragments. Thus, the reaction of [Au(SC<sub>6</sub>F<sub>5</sub>)(PPh<sub>2</sub>py)] with 1 or 2 equiv of [Au(OTf)(PPh<sub>2</sub>py)] leads to the dinuclear [Au<sub>2</sub>(μ-SC<sub>6</sub>F<sub>5</sub>)(PPh<sub>2</sub>py)<sub>2</sub>OTf (4) or the trinuclear [Au<sub>3</sub>(μ<sub>3</sub>-SC<sub>6</sub>F<sub>5</sub>)(PPh<sub>2</sub>py)<sub>3</sub>](OTf)<sub>2</sub> (5) species. The <sup>31</sup>P{<sup>1</sup>H} NMR spectra show a unique resonance for the equivalent phosphorus atoms at 32.70 and 31.64 ppm, respectively, with a downfield chemical shift for a further AuPPh<sub>2</sub>py<sup>+</sup> fragment coordinated to the sulfur atom. This trend has been previously observed in gold complexes with sulfide bridging ligands.<sup>14</sup> The <sup>19</sup>F NMR spectra exhibit the three typical resonances for a pentafluorophenyl ring. The mass spectrum for complex 4 shows the cation molecular peak [Au<sub>2</sub>(μ-SC<sub>6</sub>F<sub>5</sub>)(PPh<sub>2</sub>py)<sub>2</sub>]<sup>+</sup> at *m/z* = 1120 (55%), whereas no peaks of representative fragments are observed in the mass spectrum of 5.

Complexes [Au(SC<sub>6</sub>F<sub>5</sub>)(P–N)] are very versatile building blocks in the construction of polynuclear derivatives. They possess a heterofunctional phosphine ligand that can coordinate to other metal fragments, and the pentafluorophenyl thiolate ligand can coordinate more metal centers, as we have observed in the preparation of the doubly or triply bridging thiolate ligands in compounds 4 and 5. Therefore the reactions of complexes 1–3 with silver or copper compounds have been studied in different molar ratios. The reaction of [Au(SC<sub>6</sub>F<sub>5</sub>)(P–N)] with Ag(OTf) in a 1:1 molar ratio affords complexes with stoichiometry [AuM(μ-SC<sub>6</sub>F<sub>5</sub>)(P–N)OTf (P–N = PPh<sub>2</sub>py (6), PPh<sub>2</sub>CH<sub>2</sub>CH<sub>2</sub>py (7), or PPhpy<sub>2</sub> (8)). Complexes 6–8 show only one resonance in their <sup>31</sup>P{<sup>1</sup>H} NMR spectra, indicating the presence of either a unique phosphine or equivalent phosphine groups. Similarly, the <sup>1</sup>H NMR spectrum presents the typical resonances arising from the phosphine, and the <sup>19</sup>F NMR spectra show only one type of pentafluorophenyl ring. It is noticeable, in the case of compound 8 where both pyridine groups are equivalent, that possibly no coordination of the nitrogen atoms occurs, both of them are simultaneously bonded to the metal, or there is a fluxional behavior (Scheme 1). The LSIMS present the

Scheme 1<sup>a</sup>

<sup>a</sup> (i) K<sub>2</sub>CO<sub>3</sub>, (ii) [Au(OTf)(PPh<sub>2</sub>py)], (iii) 2 [Au(OTf)(PPh<sub>2</sub>py)], (iv) Ag(OTf) or [Cu(NCMe)<sub>4</sub>]PF<sub>6</sub>, (v) 1/2 Ag(OTf) or [Cu(NCMe)<sub>4</sub>]PF<sub>6</sub>, (vi) 4/3 Ag(OTf) or [Cu(NCMe)<sub>4</sub>]PF<sub>6</sub>, -M(SC<sub>6</sub>F<sub>5</sub>).

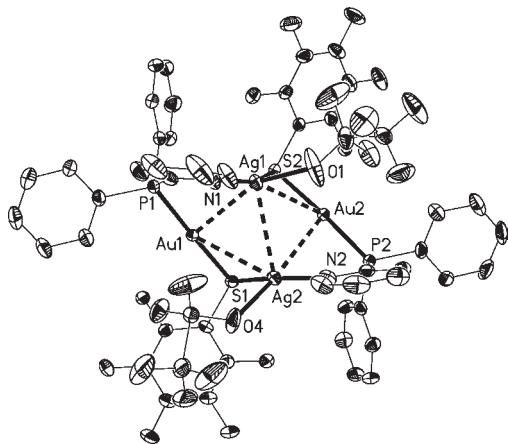


**Figure 2.** Structure of complex 6 showing the atom numbering scheme. Displacement parameter ellipsoids represent 50% probability surfaces. H atoms are omitted for clarity.

peaks arising at the fragments  $[AuAg(SC_6F_5)(PPh_2py)]^+$  at  $m/z = 767$  (30%, 6),  $[AuAg(SC_6F_5)(PPh_2CH_2CH_2py)]^+$  at  $m/z = 794$  (75%, 7), and  $[AuAg(SC_6F_5)(PPhpy_2)]^+$  at  $m/z = 769$  (30%, 8). With these data, we can propose that the silver center coordinates to the metalloligand probably through the thiolate and the pyridine or pyridines of the phosphine ligands, but it is difficult to know if the metalloligand acts as a chelate or bridging ligand, thus originating monomeric or dimeric structures, respectively.

To solve this ambiguity, the crystal structures of complexes 6 and 8 have been determined by X-ray diffraction. The molecules

can be seen in Figures 2 and 3, respectively. A selection of bond lengths and angles are collected in Tables 2 and 3. Both complexes crystallize as dimers with the silver center bonded to the thiolate, to the nitrogen atoms of the pyridine groups, and to one of the oxygens of the triflate ligand. These dimeric structures are probably stabilized by the higher degree of metallophilic bonding. Complex 6 may be described as a rhomboidal unit of alternate gold and silver atoms, in which there are also alternate thiolate and 2-pyridylphosphine ligands bridging the metallic centers. There are short Au(1)⋯Ag interactions of 2.9583(5) and 3.1783(5) Å and Au(2)–Ag interactions of 3.0545(5) and 3.0481(5) Å. The distance Ag(1)⋯Ag(2) is a bit longer, 3.2003(7) Å, but can also be considered a weak bonding interaction, whereas aurophilic interactions can be precluded as the Au⋯Au distance is too long. The gold centers present an almost ideal linear geometry with S–Au–P angles of 178.14(4) and 175.92(4)°. The silver centers are tricoordinated in an approximately trigonal planar coordination geometry (not taking into account the metallophilic interactions), with the mean deviation for the plane formed by the four atoms of 0.1 Å, and the deviation of the Ag(1) center out of the plane formed by their bonding atoms is 0.27 Å. The structure of complex 8 is slightly different because of the presence of two pyridine groups in the phosphine. The four metal centers form a more asymmetric rhomboidal unit in such a way that one of the Au–Ag segments has a longer separation. The Au–Ag distances lie in the range of 3.0961(12)–3.1470(13) Å, with a very large Au(1)⋯Ag(1) distance of 3.380(1) Å. Now there is an aurophilic contact of 3.0534(8) Å, and there is not an Ag⋯Ag interaction. The silver centers are bonded to the sulfur

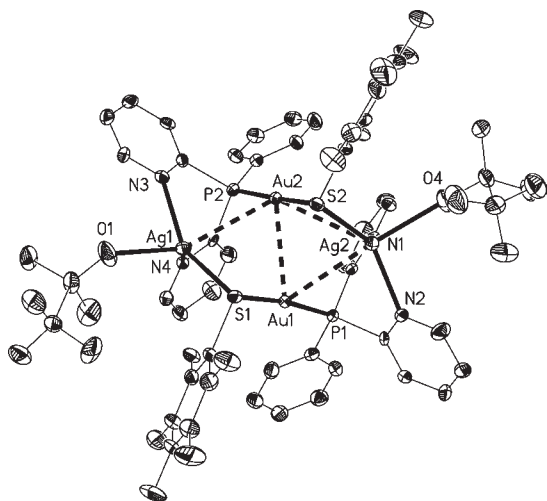


**Figure 3.** Structure of complex **8** showing the atom numbering scheme. Displacement parameter ellipsoids represent 50% probability surfaces. H atoms are omitted for clarity.

**Table 2.** Selected Bond Lengths [Å] and Angles [°] for Complex **6**<sup>a</sup>

Au(1)–P(1)	2.2591(11)	Ag(1)–N(1)	2.232(4)
Au(1)–S(1)	2.3165(10)	Ag(1)–O(1)	2.447(4)
Au(1)···Ag(1)	2.9583(5)	Ag(1)–S(2)	2.4797(11)
Au(1)···Ag(2)	3.1782(5)	Ag(1)···Ag(2)	3.2003(7)
Au(2)–P(2)	2.2583(11)	Ag(2)–N(2)	2.189(4)
Au(2)–S(2)	2.3223(11)	Ag(2)–S(1)	2.4078(11)
Au(2)···Ag(1)	3.0481(5)	Ag(2)–O(4)	2.479(4)
Au(2)···Ag(2)	3.0545(5)		

P(1)–Au(1)–S(1)	178.14(4)	N(2)–Ag(2)–S(1)	166.23(10)
P(2)–Au(2)–S(2)	175.92(4)	N(2)–Ag(2)–O(4)	89.70(14)
N(1)–Ag(1)–O(1)	87.85(14)	S(1)–Ag(2)–O(4)	100.39(11)
N(1)–Ag(1)–S(2)	154.14(11)	Au(1)–S(1)–Ag(2)	84.54(3)
O(1)–Ag(1)–S(2)	112.38(10)	Au(2)–S(2)–Ag(1)	78.73(3)

<sup>a</sup> Symmetry transformations used to generate equivalent atoms: #1  $-x + 2, -y + 2, -z + 1$ .

atom of the thiolate, to both pyridine groups, and to one of the oxygens of the triflate anion. The silver coordination geometry can be considered as very distorted tetrahedral, not taking into account the metallophilic interactions. The Ag–N distances are, for Ag(1), 2.320(9) and 2.451(10) Å, and for Ag(2), 2.312(9) and 2.405(10) Å, which are considerably longer than those found in complex **6** with a trigonal geometry. The Ag–S bond lengths are 2.480(3) and 2.452(3) Å, which are more similar to the longer ones found in complex **6** (2.4797(11) and 2.4078(11) Å).

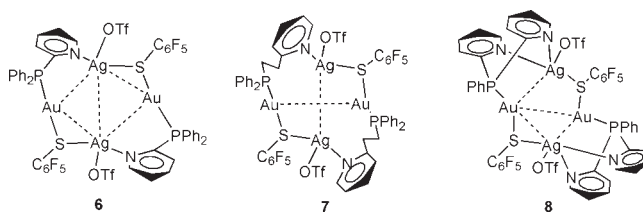
The structures found for compounds **6** and **8** and the proposed structure for complex **7** are shown in Scheme 2. As the phosphine PPh<sub>2</sub>CH<sub>2</sub>CH<sub>2</sub>py has a longer backbone, the Au···Ag distances are probably longer and some Au···Au or Ag···Ag interactions may be present.

In the same manner, the reaction of [Au(SC<sub>6</sub>F<sub>5</sub>)(P–N)] with [Cu(NCMe)<sub>4</sub>]PF<sub>6</sub> in a 1:1 molar ratio affords complexes with stoichiometry [AuCu(μ–SC<sub>6</sub>F<sub>5</sub>)(P–N)(NCMe)]PF<sub>6</sub> (P–N = PPh<sub>2</sub>py (**9**), PPh<sub>2</sub>CH<sub>2</sub>CH<sub>2</sub>py (**10**), or PPhpy<sub>2</sub> (**11**)). The

**Table 3.** Selected Bond Lengths [Å] and Angles [°] for Complex **8**

Au(1)–P(1)	2.278(3)	Ag(1)–N(3)	2.320(9)
Au(1)–S(1)	2.348(3)	Ag(1)–O(1)	2.431(10)
Au(1)···Au(2)	3.0534(8)	Ag(1)–N(4)	2.451(10)
Au(1)···Ag(2)	3.0961(12)	Ag(1)–S(1)	2.480(3)
Au(2)–P(2)	2.275(3)	Ag(2)–N(2)	2.312(9)
Au(2)–S(2)	2.336(3)	Ag(2)–N(1)	2.405(10)
Au(2)···Ag(1)	3.1165(13)	Ag(2)–O(4)	2.443(9)
Au(2)···Ag(2)	3.1470(13)	Ag(2)–S(2)	2.452(3)
P(1)–Au(1)–S(1)	171.68(10)	N(2)–Ag(2)–N(1)	84.6(3)
P(2)–Au(2)–S(2)	174.30(10)	N(2)–Ag(2)–O(4)	97.8(3)
N(3)–Ag(1)–O(1)	88.0(3)	N(1)–Ag(2)–O(4)	86.9(4)
N(3)–Ag(1)–N(4)	81.9(3)	N(2)–Ag(2)–S(2)	137.6(2)
O(1)–Ag(1)–N(4)	116.7(3)	N(1)–Ag(2)–S(2)	127.7(2)
N(3)–Ag(1)–S(1)	147.3(3)	O(4)–Ag(2)–S(2)	109.2(3)
O(1)–Ag(1)–S(1)	101.5(2)	Au(1)–S(1)–Ag(1)	88.84(10)
N(4)–Ag(1)–S(1)	119.5(2)	Au(2)–S(2)–Ag(2)	82.16(9)

**Scheme 2.** Structure of the Gold–Silver Complexes



<sup>31</sup>P{<sup>1</sup>H} NMR spectra show in all the cases one unique resonance indicating the equivalence of the phosphorus atoms, and the <sup>19</sup>F NMR spectra shows the presence of only one type of pentafluorophenyl unit. The <sup>1</sup>H NMR spectra present, in addition to the resonances due to the corresponding phosphine ligand, one singlet assigned to an acetonitrile molecule. The mass spectra (LSIMS) show the cationic peaks for [AuCu(SC<sub>6</sub>F<sub>5</sub>)(PPh<sub>2</sub>py)]<sup>+</sup> at *m/z* = 723 (100%, **9**), [AuCu(SC<sub>6</sub>F<sub>5</sub>)(PPh<sub>2</sub>CH<sub>2</sub>CH<sub>2</sub>py)]<sup>+</sup> at *m/z* = 750 (100%, **10**), and [AuAg(SC<sub>6</sub>F<sub>5</sub>)(PPhpy<sub>2</sub>)]<sup>+</sup> at *m/z* = 725 (40%, **11**). We also propose the formation of dimers for all these complexes (see Scheme 3), as has been confirmed by the X-ray diffraction structure of complex **11** (Figure 4, Table 4). Compound **11** consists of a dimeric structure with a short aurophilic interaction of 3.0028(9) Å. The gold atoms are found in an almost ideal linear geometry with angles P–Au–S of 177.38(4)° and 177.42(4)°. The copper atoms are located far from the gold centers, with distances ranging from 3.461 to 3.708 Å, too long to consider any bonding interaction. They are bonded to two nitrogen atoms of the phosphine, to the thiolate sulfur atom, and to one molecule of acetonitrile, thus rendering a slightly distorted tetrahedral geometry.

Reactions of [Au(SC<sub>6</sub>F<sub>5</sub>)(PPh<sub>2</sub>py)] with other molar ratios of Ag(OTf) or [Cu(NCMe)<sub>4</sub>]PF<sub>6</sub> have been carried out. When in a 2:1 molar ratio, the reaction affords the trinuclear derivatives [Au<sub>2</sub>M(μ–SC<sub>6</sub>F<sub>5</sub>)<sub>2</sub>(μ–PPh<sub>2</sub>py)<sub>2</sub>]X (M = Ag, X = OTf (**12**); M = Cu, X = PF<sub>6</sub> (**13**)) in high yield. The <sup>31</sup>P{<sup>1</sup>H} NMR spectra show the presence of equivalent phosphorus atoms, and the <sup>19</sup>F and

Scheme 3. Structure of the Gold–Copper Complexes

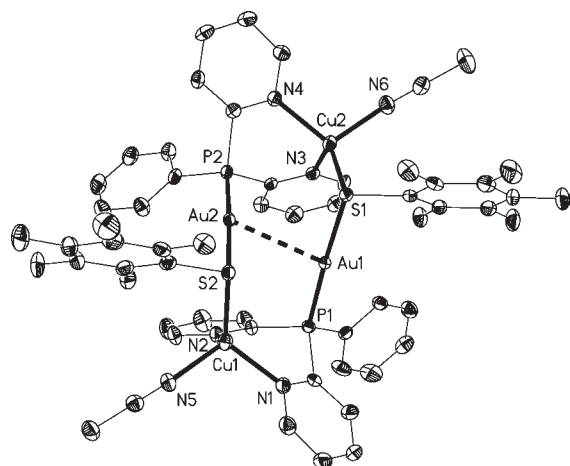
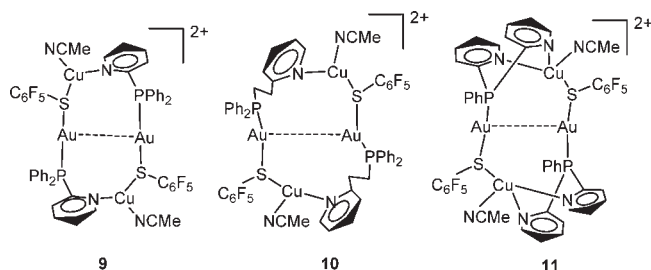


**Figure 4.** Structure of the cation of complex **9** showing the atom numbering scheme. Displacement parameter ellipsoids represent 50% probability surfaces. H atoms are omitted for clarity.

$^1\text{H}$  NMR spectra display only one type of pentafluorophenyl ring or diphenylphosphinopyridine ligand, respectively. It has not been possible to study these complexes by X-ray diffraction, but according to the NMR data the proposed structure consists of a trinuclear derivative, in which the silver or copper atoms are in a tetrahedral geometry, bonded to a chelate metalloligand  $[\text{Au}(\text{SC}_6\text{F}_5)(\text{PPh}_2\text{py})]$  through the pyridine and the sulfur atoms (see Scheme 1).

Finally, the reaction of  $[\text{Au}(\text{SC}_6\text{F}_5)(\text{PPh}_2\text{py})]$  with  $\text{Ag}(\text{OTf})$  or  $[\text{Cu}(\text{NCMe})_4]\text{PF}_6$  in a 4:3 molar ratio has also been carried out and occurs with the precipitation of insoluble  $\text{M}(\text{SC}_6\text{F}_5)$  and the formation of complexes with stoichiometry  $[\text{Au}_4\text{M}_2(\mu\text{-SC}_6\text{F}_5)_3(\mu\text{-PPh}_2\text{py})_4]\text{X}_3$  ( $\text{M} = \text{Ag}$ ,  $\text{X} = \text{OTf}$  (**14**);  $\text{M} = \text{Cu}$ ,  $\text{X} = \text{PF}_6$  (**15**)). The  $^{31}\text{P}\{^1\text{H}\}$  NMR spectrum of **15** shows a unique resonance, even at low temperature, for the phosphorus atoms, which indicates the equivalence of the phosphine ligands or a rapid exchange process in the NMR time scale. More surprisingly, the  $^{19}\text{F}$  NMR spectrum of **15** presents the three typical resonances (2:2:1 ratio) of equivalent pentafluorophenyl groups, but the low temperature spectra show a different pattern, and three different pentafluorophenyl groups, as expected for the proposed product, were observed. The NMR data for complex **14** show a mixture of products, but the resonances for **14** could be assigned.

The structure of complex **15** has been established by an X-ray diffraction study, and a simplified representation of the cation is shown in Figure 5. A selection of bond lengths and angles are

**Table 4.** Selected Bond Lengths [ $\text{\AA}$ ] and Angles [ $^\circ$ ] for Complex **11**

Au(1)–P(1)	2.2700(14)	Cu(1)–N(2)	2.078(4)
Au(1)–S(1)	2.3383(14)	Cu(1)–S(2)	2.2726(15)
Au(1)···Au(2)	3.0028(9)	Cu(2)–N(6)	2.006(5)
Au(2)–P(2)	2.2640(13)	Cu(2)–N(4)	2.051(4)
Au(2)–S(2)	2.3310(13)	Cu(2)–N(3)	2.078(4)
Cu(1)–N(5)	2.003(4)	Cu(2)–S(1)	2.2815(14)
Cu(1)–N(1)	2.039(4)		

P(1)–Au(1)–S(1)	177.38(4)	N(6)–Cu(2)–N(4)	106.84(18)
P(2)–Au(2)–S(2)	177.42(4)	N(6)–Cu(2)–N(3)	110.44(17)
N(5)–Cu(1)–N(1)	107.83(17)	N(4)–Cu(2)–N(3)	95.66(16)
N(5)–Cu(1)–N(2)	105.11(17)	N(6)–Cu(2)–S(1)	105.02(13)
N(1)–Cu(1)–N(2)	95.62(16)	N(4)–Cu(2)–S(1)	122.05(12)
N(5)–Cu(1)–S(2)	108.24(13)	N(3)–Cu(2)–S(1)	116.36(12)
N(1)–Cu(1)–S(2)	119.95(12)	Cu(2)–S(1)–Au(1)	97.01(6)
N(2)–Cu(1)–S(2)	118.62(13)	Cu(1)–S(2)–Au(2)	97.91(6)

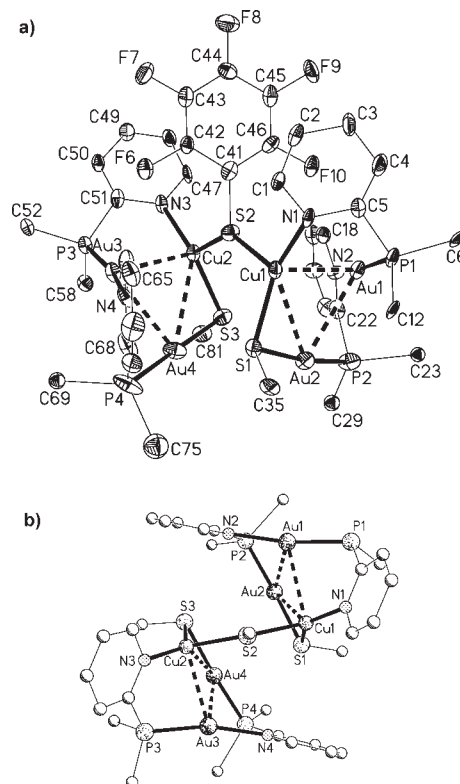


**Figure 5.** (a) A simplified representation of the molecular structure of complex **15** (for clarity only the ipso carbon atoms have been represented for all phenyl rings and for two of the pentafluorophenyl rings). (b) Schematic representation of the central metal skeleton (all phenyl rings represented only by their ipso carbon).

collected in Table 5. The structure shows two trinuclear, structurally different  $[\text{Au}_2\text{Cu}(\text{SC}_6\text{F}_5)(\text{PPh}_2\text{py})_2]$  units bridged by a third  $\mu\text{-S}$ -pentafluorophenyl thiolate group, which is bonded to the two copper atoms. The two trinuclear units consist of asymmetric  $\text{Au}_2\text{Cu}$  triangles with relatively short distances among the metals:  $\text{Au}\cdots\text{Au}$  in the range of 2.9716(12)–2.9898(11)  $\text{\AA}$ ,

**Table 5. Selected Bond Lengths [Å] and Angles [°] for the Cationic Complex of 15**

Au(1)···Au(2)	2.9898(11)	Au(3)···Au(4)	2.9716(12)
Au(1)···Cu(1)	2.930(2)	Au(3)···Cu(2)	2.870(2)
Au(1)–P(1)	2.245(4)	Au(3)–P(3)	2.239(4)
Au(1)–N(2)	2.110(13)	Au(3)–N(4)	2.148(12)
Au(2)···Cu(1)	3.233(2)	Au(4)···Cu(2)	3.028(2)
Au(2)–P(2)	2.267(5)	Au(4)–P(4)	2.258(6)
Au(2)–S(1)	2.317(4)	Au(4)–S(3)	2.329(5)
Cu(1)–S(1)	2.215(5)	Cu(2)–S(3)	2.240(5)
Cu(1)–S(2)	2.277(4)	Cu(2)–S(2)	2.245(4)
Cu(1)–N(1)	1.980(14)	Cu(2)–N(3)	1.988(12)
<hr/>			
P(1)–Au(1)–N(2)	170.4(4)	P(3)–Au(3)–N(4)	166.3(4)
P(2)–Au(2)–S(1)	171.93(17)	P(4)–Au(4)–S(3)	176.23(19)
S(1)–Cu(1)–S(2)	107.63(17)	S(3)–Cu(2)–S(2)	107.50(18)
S(1)–Cu(1)–N(1)	142.3(3)	S(3)–Cu(2)–N(3)	134.2(4)
S(2)–Cu(1)–N(1)	107.7(3)	S(2)–Cu(2)–N(3)	114.6(4)
Au(2)–S(1)–Cu(1)	90.98(15)	Au(4)–S(3)–Cu(2)	83.01(17)
Cu(1)–S(2)–Cu(2)	137.3(2)		

while the Au···Cu exhibits two different separations, one in the range of 2.870–2.930(2) Å and a second one clearly longer at 3.028–3.233(2) Å. The gold centers are bridged by a  $\kappa$ -N,P-PPh<sub>2</sub>py ligand, one Au···Cu pair is bridged by another  $\kappa$ -N,P-PPh<sub>2</sub>py ligand, and the second Au···Cu side is bridged by a SC<sub>6</sub>F<sub>5</sub> ligand.

**DRUV and Luminescence Studies.** The diffuse reflectance UV (DRUV) spectra of solid samples of complexes **1–15** have been recorded. All of them display broad bands. In most cases the band profile shows two maxima, which are not always well-defined. One of these maxima appears at about 250 nm and the other at about 350 nm (Table 6). This behavior is illustrated in Figure 6. In some other cases a third maximum is observed. An absorption band in dichloromethane solutions at 261 nm in the UV spectra of PPh<sub>2</sub>py has been attributed to intraligand  $\pi \rightarrow \pi$  or  $n \rightarrow \pi$  transitions. The less intense broad shoulders observed in our complexes include energies that have been assigned to thiolate IL transitions or <sup>3</sup>LMCT transitions in other thiolate–gold complexes.<sup>10,15</sup>

The excitation and emission spectra of [Au<sub>4</sub>Ag<sub>2</sub>( $\mu$ -SC<sub>6</sub>F<sub>5</sub>)<sub>3</sub>( $\mu$ -PPh<sub>2</sub>py)<sub>4</sub>](OTf)<sub>3</sub> (**14**) have not been studied, as it is obtained as a mixture of products. The rest of the complexes are emissive. They display weak emissions, and some of them are only luminescent at low temperature. At 77 K two bands are observed for most of the complexes: an example is shown in Figure 7. When two maxima are not distinguished, very broad bands are found. Thus, for the cases in which we have obtained a lifetime for the two different emissions, they are shown in Table 6. They lie between 2 and 17  $\mu$ s, which could point to a phosphorescence nature of the emissions. In order to propose an origin for these emissions, we will first analyze the metalloligands (**1–3**) as well as the polygold derivatives (**4** and **5**), and then we will study the influence of the heterometal in the polyheterometallic complexes (**6–13** and **15**).

**Metalloligands.** The emissions observed for complexes [Au(SC<sub>6</sub>F<sub>5</sub>)(P–N)] (**1–3**) could be attributed to intraligand (IL) monophosphine based transitions or ligand (chalcogenolate) to metal charge transfer (LMCT) transitions. The latter are widely

represented among chalcogenolate luminescent complexes.<sup>15</sup> The free monophosphines are emissive,<sup>10,16</sup> for which we have observed emissions at 314 and 375 at 554 nm (PPh<sub>2</sub>py) and 443 nm (PPh<sub>2</sub>CH<sub>2</sub>CH<sub>2</sub>py) at room temperature and 529 (PPh<sub>2</sub>py), 491 nm (PPh<sub>2</sub>CH<sub>2</sub>CH<sub>2</sub>py), and 499 nm (PPhpy<sub>2</sub>) at 77 K. These emissions are very close in energy to those corresponding to the high energy band displayed at 77 K by complexes **1–3**; thus, we can tentatively propose an intraligand (monophosphine) origin for this band, modified upon coordination to the gold center. The gold complexes [AuCl(P–N)] (P–N = PPh<sub>2</sub>py and PPhpy<sub>2</sub>) display emissions at 499 nm at 77 K and are not emissive at room temperature. An IL origin has been assigned to these emissions,<sup>17</sup> which show a smaller shift of the emission energy compared with that found in the free phosphines. The band at lower energies found in **1** and **2** at 77 K probably arises from <sup>3</sup>LMCT (C<sub>6</sub>F<sub>5</sub>S  $\rightarrow$  Au) transitions. The influence of the presence of aurophilic interactions in the emission energy in thiolate-to-gold charge transfer transitions has been reported.<sup>15a</sup> This study concludes that a red shift of the emission maxima is observed when such interactions are present. Another conclusion is that the emission energy, as unique data, is not enough to postulate the presence of aurophilic interactions.

The di- and trinuclear gold species [Au<sub>x</sub>( $\mu$ -SC<sub>6</sub>F<sub>5</sub>)(PPh<sub>2</sub>py)<sub>x</sub>](OTf)<sub>n</sub> (**4**:  $x = 2$ ,  $n = 1$ ; **5**:  $x = 3$ ,  $n = 2$ ) display two emissions at low temperature for which we postulate the origins commented above. A mixed metal centered  $Sd(d\sigma^*) \rightarrow 6p(p\sigma)$  and <sup>3</sup>LMCT S  $\rightarrow$  Au character has been proposed for the emission at 640 nm observed in [Au<sub>2</sub>(8-Squin)(PPh<sub>3</sub>)<sub>2</sub>]BF<sub>4</sub> (Squin = quinoline-8-thiolate).<sup>15b</sup> A metal-centered contribution could be also postulated for the low energy emissions found in **4** and **5**, for which the presence of gold···gold interactions is expected.

**Heterometallic Complexes.** At room temperature almost all the complexes display emission maxima at  $\lambda \geq 600$  nm. At 77 K a very broad band or two bands are observed (Table 6). Two emissions have been observed for some compounds upon changing the excitation energy. Figure 8 illustrates this behavior for compound **13**. When very broad bands are obtained, a unique maxima and the width of the band are given in Table 6. As two emissions with different degrees of resolution are generally present, we will discuss first the one at higher energy and then the one at lower energy.

For the heterometallic gold/silver and gold/copper complexes, we propose that the emissions at high energy arise from IL transitions, as discussed above. The band at low energy appears at lower wavelengths for the copper/gold complexes compared with the analogous silver/gold complexes of stoichiometry: [Au<sub>2</sub>M<sub>2</sub>( $\mu$ -SC<sub>6</sub>F<sub>5</sub>)<sub>2</sub>(NCMe)<sub>2</sub>( $\mu$ -P–N)<sub>2</sub>] X<sub>2</sub> (M = Ag, X = OTf<sup>–</sup>; M = Cu, X = PF<sub>6</sub><sup>–</sup>). This fact indicates that there is an influence of the heterometal in the emission energy. As different emission energies are observed depending on the heterometal (silver or copper), this fact could serve as a tentative test in order to know which heterometal has been coordinated.

The trend may be resumed as follows: in the silver/gold complexes this band appears at  $\lambda > 700$  nm, in the red region, whereas in the copper/gold complexes it is at  $\lambda < 650$  nm and results in an orange or pale red emission. We propose a <sup>3</sup>LMCT origin for this band. The crystal structures reveal very different patterns of metallic interactions; for instance, the structure of compound **11** displays aurophilic but not Cu···Au interactions. The silver/gold complexes display more complicated structures, which involve Ag···Ag and Ag···Au interactions. Complex **6**

Table 6. Luminescence and DRUV Data for Complexes 1–15

	298 K <sup>a</sup>	77 K <sup>a</sup>	$\tau$ ( $\mu$ s) <sup>b</sup>	DRUV/in nm <sup>c</sup>
[Au(SC <sub>6</sub> F <sub>5</sub> )(P–N)]				
PPh <sub>2</sub> py (1)	535 (430)	530 (400) <b>598</b> (360)		[230–400] <b>250</b> , <b>340</b>
PPh <sub>2</sub> CH <sub>2</sub> CH <sub>2</sub> py (2)	584 (400)	568 (400)	12	[210–430] <b>260</b> ; <b>330</b>
PPhpy <sub>2</sub> (3)		<b>574</b> (350) 650 (400)		[230–350] <b>260</b> , <b>310</b>
[Au <sub>2</sub> ( $\mu$ -SC <sub>6</sub> F <sub>5</sub> )(PPh <sub>2</sub> py) <sub>2</sub> ](OTf) (4)	broad band [450–725] 582 370	broad band 507 (370) 601 (370)	17.6, 10	250; 310–450 (br)
[Au <sub>3</sub> ( $\mu$ -C <sub>6</sub> F <sub>5</sub> )(PPh <sub>2</sub> py) <sub>3</sub> ](OTf) <sub>2</sub> (5)	broad band [430–650] 501 370	broad band 465 (320) 588 (379)		240; 310–410 (br)
[Ag <sub>2</sub> Au <sub>2</sub> ( $\mu$ -SC <sub>6</sub> F <sub>5</sub> ) <sub>2</sub> (OTf) <sub>2</sub> ( $\mu$ -P–N) <sub>2</sub> ]				
PPh <sub>2</sub> py (6)		<b>531</b> (360) 740 (422)		[225–430] <b>250</b> ; 330, 400
PPh <sub>2</sub> CH <sub>2</sub> CH <sub>2</sub> py (7)	745 (450)	707 (420)	8.5	[210–380] <b>260</b> ; 300
PPhpy <sub>2</sub> (8)		broad band <b>584</b> (350) 658 (400)		[230–420] <b>260</b> ; <b>330</b>
[Au <sub>2</sub> Cu <sub>2</sub> ( $\mu$ -SC <sub>6</sub> F <sub>5</sub> ) <sub>2</sub> (NCMe) <sub>2</sub> ( $\mu$ -P–N) <sub>2</sub> ](PF <sub>6</sub> ) <sub>2</sub>				
PPh <sub>2</sub> py (9)	600 (430)	broad band [450–725] 573	16.6, 7.1	[210–450] <b>260</b> ; <b>340</b>
PPh <sub>2</sub> CH <sub>2</sub> CH <sub>2</sub> py (10)		557 (370) 629 (450)		[210–400]
PPhpy <sub>2</sub> (11)		broad band <b>557</b> (370) 635 (450)		[230–530] <b>260</b> , <b>340</b> , <b>410</b>
[AgAu <sub>2</sub> ( $\mu$ -SC <sub>6</sub> F <sub>5</sub> ) <sub>2</sub> ( $\mu$ -PPh <sub>2</sub> py) <sub>2</sub> ](OTf) (12)		broad band [430–750] 569 (370–440)		[210–410] <b>275</b> ; <b>325</b>
[Au <sub>2</sub> Cu( $\mu$ -SC <sub>6</sub> F <sub>5</sub> ) <sub>2</sub> ( $\mu$ -PPh <sub>2</sub> py) <sub>2</sub> ](PF <sub>6</sub> ) (13)	600 (430)	broad band 567 (370) 632 (440)	10.9, 2.8	[210–450] <b>260</b> ; <b>335</b>
[Au <sub>4</sub> Cu <sub>2</sub> ( $\mu$ -SC <sub>6</sub> F <sub>5</sub> ) <sub>3</sub> ( $\mu$ -PPh <sub>2</sub> py) <sub>4</sub> ](PF <sub>6</sub> ) <sub>3</sub> (15)	620 (420)	broad band <b>583</b> (400) 658 (425)	12.8, 2.0	[210–450] <b>260</b> ; <b>335</b>

<sup>a</sup>  $\lambda_{\text{MAXIMUM}}$  of emission ( $\lambda_{\text{MAXIMUM}}$  of excitation) in nm. When two maxima are observed the most intense one is shown in bold. When only a very broad band is observed: [range], maximum of emission and (range of excitation) are shown. <sup>b</sup> At room temperature. <sup>c</sup> [Range of the broad band] maxima observed (that with higher intensity is in bold).

displays Ag···Ag interactions, and complex **8** displays Au···Au contacts. Thus, the participation of the heterometal in a concrete sort of metallic interaction seems not to be the cause of the different emission maxima. Nevertheless, the influence of the heterometal is clear, and thus probably the origin of this band is a chalcogenolate to gold/heterometal charge transfer transition that could be represented as <sup>3</sup>LAuMCT (RS → Au/M). The presence of silver leads, in general, to emissions at lower energies than the coordination of copper. As discussed above, in some occasions one broad emission is observed, which possibly has a mixture IL and <sup>3</sup>LAuMCT (RS → Au/M) character.

## CONCLUSIONS

The metalloligand complexes [Au(SC<sub>6</sub>F<sub>5</sub>)(P–N)] (P–N = PPh<sub>2</sub>py, PPh<sub>2</sub>CH<sub>2</sub>CH<sub>2</sub>py, or PPhpy<sub>2</sub>) have been prepared and used as building blocks to construct unprecedented heterometallic aggregates by reaction with silver(I) or copper(I) compounds. In the reactions with a 1:1 molar ratio, these aggregates are dimers that present an Au<sub>2</sub>Ag<sub>2</sub> or Au<sub>2</sub>Cu<sub>2</sub> core, which allows the presence of different metallophilic interactions. Other molar ratios have been used, such as 2:1 or 3:4, giving complexes with chelate or triply bridging metalloligands as [Au<sub>2</sub>M( $\mu$ -SC<sub>6</sub>F<sub>5</sub>)<sub>2</sub>( $\mu$ -P–N)<sub>2</sub>]X or [Au<sub>4</sub>M<sub>2</sub>( $\mu$ -SC<sub>6</sub>F<sub>5</sub>)<sub>3</sub>( $\mu$ -P–N)<sub>4</sub>]X<sub>3</sub>, respectively.

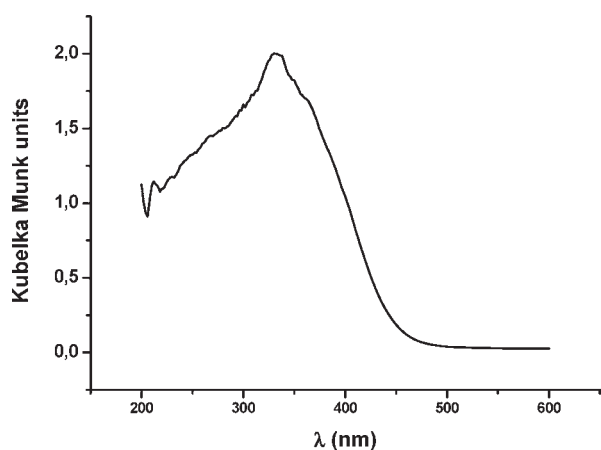


Figure 6. DRUV spectrum of compound 6.

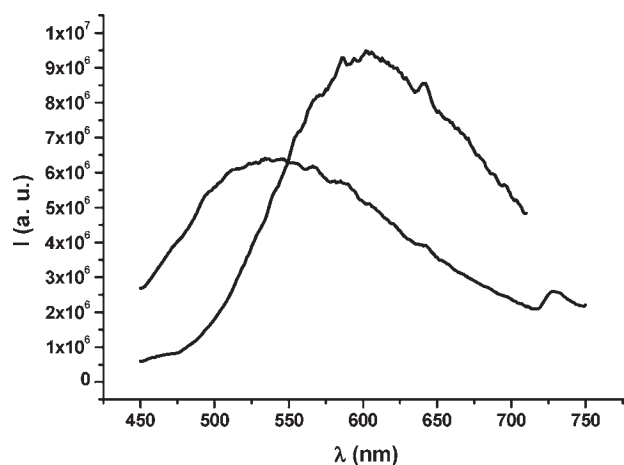


Figure 7. Two emission maxima observed in 1.

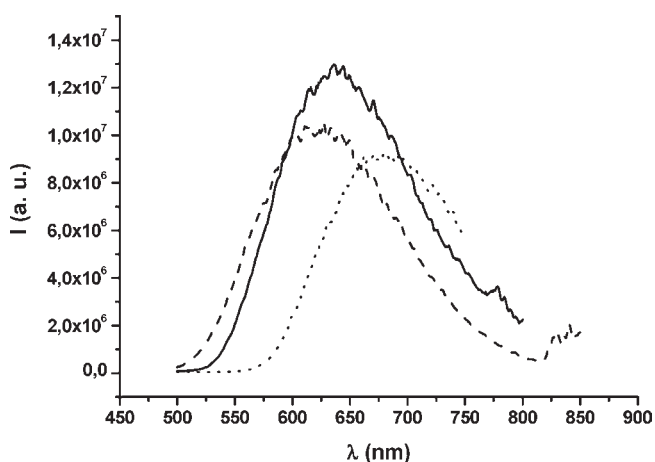


Figure 8. Emission observed in 13. A broad band (straight line) may be split into two emissions upon changing the excitation maximum ( $\lambda = 350$  nm, dotted line; 450 nm, dashed line).

The complexes display weak emissions, and some of them are only luminescent at low temperature. At 77 K, two bands are observed for most of the complexes. The lifetime values in the

microsecond range point to a phosphorescent nature of the luminescence. At 77 K, a very broad band or two bands are observed for most of the complexes. The one at high energy probably arises from IL (monophosphine) transitions. A  $^3\text{LMCT}$  ( $\text{S} \rightarrow \text{Au}$ ) origin is proposed for the low energy band for the metalloligands 1–3. In the heterometallic complexes, the influence of the heterometal leads to different energy emissions. In general, silver/copper complexes exhibit this band at lower energies than the homologous copper complexes. This interesting fact may tentatively be used to identify the heterometal in such species. The nature of this band has been proposed as  $^3\text{LAuMCT}$  ( $\text{S} \rightarrow \text{AuM}$ ). Although further studies focused on these systems are required, this work could be the starting point for preparing intense luminescent heteropolynuclear complexes. The luminescence of such complexes would depend on the heterometal, and thus the complexes would serve as a probe or sensor for the heterometal.

## EXPERIMENTAL SECTION

**Instrumentation.** Infrared spectra were recorded in the range of 4000–200  $\text{cm}^{-1}$  on a Perkin–Elmer 883 spectrophotometer using Nujol mulls between polyethylene sheets. C, H, N, and S analyses were carried out with a Perkin–Elmer 2400 microanalyzer. Mass spectra were recorded on a VG Autospec, with the LSIMS technique, using nitrobenzyl alcohol as matrix. NMR spectra were recorded on a Bruker ARX 300 or a Bruker AV 400 spectrometer. Chemical shifts are cited relative to  $\text{SiMe}_4$  ( $^1\text{H}$ , external) and 85%  $\text{H}_3\text{PO}_4$  ( $^{31}\text{P}$ , external). DRUV spectra were recorded with a UnicamUV-4 spectrophotometer equipped with a Spectralon RSA-UC-40 Labsphere integrating sphere. The solid samples were mixed with dried KBr and placed in a homemade cell equipped with a quartz window. The intensities were recorded in Kubelka–Munk units:  $(1 - R)^2/2R$ , where  $R$  = reflective index. Steady-state photoluminescence spectra were recorded with a Jobin–Yvon Horiba Fluorolog FL-3-11 spectrometer using band pathways of 3 nm both for excitation and emission. Phosphorescence lifetimes were recorded with a Fluoromax phosphorimeter accessory containing a UV xenon flash tube. The lifetime data were fit using the Jobin–Yvon software package<sup>18</sup> and the Origin 5.0 program.<sup>19</sup>

**Starting Materials.** The starting materials  $\text{PPh}_2\text{CH}_2\text{CH}_2\text{py}$ ,<sup>20</sup>  $\text{PPhpy}_2$ ,<sup>21</sup>  $[\text{AuCl}(\text{PPh}_2\text{py})]$ ,<sup>22</sup>  $[\text{AuCl}(\text{PPh}_2\text{CH}_2\text{CH}_2\text{py})]$ ,<sup>17</sup> and  $[\text{Cu}(\text{NCMe})_4]\text{PF}_6$ <sup>23</sup> were prepared according to published procedures. All other reagents were commercially available.  $[\text{Au}(\text{OTf})(\text{PPh}_2\text{py})]$  was prepared from the reaction of  $[\text{AuCl}(\text{PPh}_2\text{py})]$  with  $\text{Ag}(\text{OTf})$  in dichloromethane and used in situ.

**Synthesis of  $[\text{Au}(\text{SC}_6\text{F}_5)(\text{P}-\text{N})]$  ( $\text{P}-\text{N} = \text{PPh}_2\text{py}$  (**1**),  $\text{PPh}_2\text{CH}_2\text{CH}_2\text{py}$  (**2**), or  $\text{PPhpy}_2$  (**3**)).** To a solution of  $[\text{AuCl}(\text{PPh}_2\text{py})]$  (0.495 g, 1 mmol),  $[\text{AuCl}(\text{PPh}_2\text{CH}_2\text{CH}_2\text{py})]$  (0.523 g, 1 mmol), or  $[\text{AuCl}(\text{PPhpy}_2)]$  (0.497 g, 1 mmol) in 15 mL of dichloromethane under nitrogen atmosphere were added  $\text{HSC}_6\text{F}_5$  (0.14 mL, 1 mmol) and  $\text{K}_2\text{CO}_3$  in excess. The mixture was stirred at room temperature for 2 h. After this time it was filtered through Celite to remove the precipitate. The resulting solution was concentrated to 5 mL and  $\text{Et}_2\text{O}$  was added, giving a white solid of **1** (0.262 g, 80%), a white solid of **2** (0.165 g, 49%), or an orange solid of **3** (0.251 g, 76%). **Complex 1:** Anal. Calcd. for  $\text{C}_{23}\text{H}_{19}\text{AuF}_5\text{NPS}$  (MW = 659.36): C, 41.89; H, 2.14; N, 2.12; S, 4.86. Found: C, 41.56; H, 1.83; N, 2.52; S, 4.46. MS(LSIMS+):  $m/z = 660$  (15%,  $[\text{Au}(\text{SC}_6\text{F}_5)(\text{PPh}_2\text{py})]$ ).  $^{31}\text{P}\{^1\text{H}\}$  NMR ( $\text{CDCl}_3$ , ppm): 36.6 (s, 2P,  $\text{PPh}_2\text{py}$ ).  $^1\text{H}$  NMR ( $\text{CDCl}_3$ , ppm): 8.80 (d, 1H, py,  $^3J_{\text{H}-\text{H}} = 4.6$  Hz), 7.91 (t, 1H, py,  $^3J_{\text{H}-\text{H}} = 7.6$  Hz), 7.82–7.45 (m, 10 + 1H, Ph + py), 7.39 (m, 1H, py).  $^{19}\text{F}$  NMR ( $\text{CDCl}_3$ , ppm): –132.33 (m, 2F, *o*-F), –162.48 (t, 1F, *p*-F,  $^2J_{\text{F}-\text{F}} = 21$  Hz), –164.13 (m, 2F, *m*-F). **Complex 2:** Anal. Calcd. for  $\text{C}_{25}\text{H}_{18}\text{AuF}_5\text{NPS}$  (MW = 687.41): C, 43.68; H, 2.64; N,



2.03; S, 4.66. Found: C, 43.38; H, 2.77; N, 2.16; S, 4.76. MS(LSIMS+):  $m/z = 688$  (17%,  $[\text{Au}(\text{SC}_6\text{F}_5)(\text{PPh}_2\text{CH}_2\text{CH}_2\text{py})]$ ).  $^{31}\text{P}\{^1\text{H}\}$  NMR ( $(\text{CD}_3)_2\text{CO}$ , ppm): 35.6 (s, 2P,  $\text{PPh}_2\text{CH}_2\text{CH}_2\text{py}$ ).  $^1\text{H}$  NMR ( $(\text{CD}_3)_2\text{CO}$ , ppm): 8.45 (d, 1H, py,  $^3J_{\text{H-H}} = 4.8$  Hz), 7.89–7.52 (m, 10 + 1H, Ph + py), 7.26 (d, 1H, py,  $^3J_{\text{H-H}} = 7.8$  Hz), 7.16 (m, 1H, py), 3.26–3.06 (m, 4H,  $\text{CH}_2$ ).  $^{19}\text{F}$  NMR ( $(\text{CD}_3)_2\text{CO}$ , ppm): –132.91 (m, 2F, o-F), –164.53 (t, 1F, p-F,  $^2J_{\text{F-F}} = 20.6$  Hz), –165.30 (m, 2F, m-F). Complex 3: Anal. Calcd. for  $\text{C}_{22}\text{H}_{13}\text{AuF}_5\text{N}_2\text{P}_2\text{S}$  (MW = 660.35): C, 40.01; H, 1.98; N, 4.24; S, 4.84. Found: C, 40.40; H, 2.23; N, 4.32; S, 5.05. MS(LSIMS+):  $m/z = 661$  (65%,  $[\text{Au}(\text{SC}_6\text{F}_5)(\text{PPhpy}_2)]$ ).  $^{31}\text{P}\{^1\text{H}\}$  NMR ( $\text{CDCl}_3$ , ppm): 36.3 (s, P,  $\text{PPhpy}_2$ ).  $^1\text{H}$  NMR ( $\text{CDCl}_3$ , ppm): 8.75 (d, 2H, py,  $^3J_{\text{H-H}} = 4.6$  Hz), 7.97 (m, 2H, py), 7.86–7.48 (m, 5 + 2H, Ph + py), 7.37 (m, 2H, py).  $^{19}\text{F}$  NMR ( $\text{CDCl}_3$ , ppm): –132.25 (m, 2F, o-F), –162.45 (t, 1F, p-F,  $^2J_{\text{F-F}} = 19.7$  Hz), –164.13 (m, 2F, m-F).

**Synthesis of  $[\text{Au}_2(\mu\text{-SC}_6\text{F}_5)(\text{PPh}_2\text{py})_2](\text{OTf})$  (**4**).** To a solution of  $[\text{Au}(\text{OTf})(\text{PPh}_2\text{py})]$  (0.073 g, 0.12 mmol) in 20 mL of dichloromethane was added  $[\text{Au}(\text{SC}_6\text{F}_5)(\text{PPh}_2\text{py})]$  (0.066 g, 0.1 mmol), and the mixture was stirred for 1 h. The solution was concentrated to 5 mL, and the addition of  $\text{Et}_2\text{O}$  gave a white solid of **4** (0.112 g, 88%). Anal. Calcd. for  $\text{C}_{41}\text{H}_{28}\text{Au}_2\text{F}_8\text{N}_2\text{P}_4\text{O}_3\text{S}_2$  (MW = 1268.66): C, 38.80; H, 2.20; N, 2.20; S, 5.04. Found: C, 38.72; H, 2.03; N, 2.24; S, 4.99. MS(LSIMS+):  $m/z = 1120$  (55%,  $[\text{Au}_2(\text{SC}_6\text{F}_5)(\text{PPh}_2\text{py})_2]^+$ ).  $^{31}\text{P}\{^1\text{H}\}$  NMR ( $\text{CDCl}_3$ , ppm): 32.7 (s, 2P,  $\text{PPh}_2\text{py}$ ).  $^1\text{H}$  NMR ( $\text{CDCl}_3$ , ppm): 8.89 (m, 2H, py), 7.88 (m, 2H, py), 7.56–7.44 (m, 20 + 4H, Ph + py).  $^{19}\text{F}$  NMR ( $\text{CDCl}_3$ , ppm): –80.07 (s, 3F,  $\text{CF}_3\text{SO}_3$ ), –133.64 (m, 2F, o-F), –162.38 (m, 1F, p-F), –165.27 (m, 2F, m-F).

**Synthesis of  $[\text{Au}_3(\mu_3\text{-SC}_6\text{F}_5)(\text{PPh}_2\text{py})_3](\text{OTf})_2$  (**5**).** To a solution of  $[\text{Au}(\text{OTf})(\text{PPh}_2\text{py})]$  (0.133 g, 0.22 mmol) in 30 mL of dichloromethane was added  $[\text{Au}(\text{SC}_6\text{F}_5)(\text{PPh}_2\text{py})]$  (0.066 g, 0.1 mmol), and the mixture was stirred for 1 h. The solution was evaporated to 5 mL, and  $\text{Et}_2\text{O}$  was added, giving a white solid of **5** (0.137 g, 73%). Anal. Calcd. for  $\text{C}_{59}\text{H}_{42}\text{Au}_3\text{F}_{11}\text{N}_3\text{P}_3\text{S}_3\text{O}_6$  (MW = 1877.98): C, 37.71; H, 2.38; N, 2.24; S, 5.25. Found: C, 37.91; H, 2.49; N, 2.32; S, 5.20.  $^{31}\text{P}\{^1\text{H}\}$  NMR ( $\text{CDCl}_3$ , ppm): 31.6 (s, 3P,  $\text{PPh}_2\text{py}$ ).  $^1\text{H}$  NMR ( $\text{CDCl}_3$ , ppm): 8.91 (m, 3H, py), 7.90 (m, 3H, py), 7.55–7.47 (m, 30 + 6H, Ph + py).  $^{19}\text{F}$  NMR ( $\text{CDCl}_3$ , ppm): –80.11 (s, 3F,  $\text{CF}_3\text{SO}_3$ ), –133.27 (m, 2F, o-F), –161.00 (m, 1F, p-F), –164.72 (m, 2F, m-F).

**Synthesis of  $[\text{Ag}_2\text{Au}_2(\mu\text{-SC}_6\text{F}_5)_2(\text{OTf})_2(\mu\text{-P-N})_2]$  ( $P\text{-N} = \text{PPh}_2\text{py}$  (**6**),  $\text{PPh}_2\text{CH}_2\text{CH}_2\text{py}$  (**7**), or  $\text{PPhpy}_2$  (**8**)).** To a solution of  $[\text{Au}(\text{SC}_6\text{F}_5)(\text{PPh}_2\text{py})]$  (0.066 g, 0.1 mmol),  $[\text{Au}(\text{SC}_6\text{F}_5)(\text{PPh}_2\text{CH}_2\text{CH}_2\text{py})]$  (0.068 g, 0.1 mmol), or  $[\text{Au}(\text{SC}_6\text{F}_5)(\text{PPhpy}_2)]$  (0.066 g, 0.1 mmol) in 15 mL of dichloromethane was added  $\text{Ag}(\text{OTf})$  (0.025 g, 0.1 mmol). After 20 min of stirring, the mixture was filtered through Celite and the solution was evaporated to 5 mL. Addition of  $\text{Et}_2\text{O}$  gave a white solid of **6** (0.076 g, 75%). Addition of hexane afforded a white solid of **7** (0.052 g, 62%) or a yellow solid of **8** (0.066 g, 70%). Complex **6**: Anal. Calcd. for  $\text{C}_{48}\text{H}_{28}\text{Ag}_2\text{Au}_2\text{F}_{16}\text{N}_2\text{P}_2\text{O}_6\text{S}_4$  (MW = 1832.6): C, 31.45; H, 1.54; N, 1.52; S, 6.99. Found: C, 31.22; H, 1.20; N, 1.50; S, 6.73. MS(LSIMS+):  $m/z = 767$  (25%,  $[\text{AgAu}(\text{SC}_6\text{F}_5)(\text{PPh}_2\text{py})]^+$ ).  $^{31}\text{P}\{^1\text{H}\}$  NMR ( $\text{CDCl}_3$ , ppm): 39.0 (s, 2P,  $\text{PPh}_2\text{py}$ ).  $^1\text{H}$  NMR ( $\text{CDCl}_3$ , ppm): 8.99 (m, 2H, py), 8.76 (m, 2H, py), 7.84–7.04 (m, 20 + 4H, Ph + py).  $^{19}\text{F}$  NMR ( $\text{CDCl}_3$ , ppm): –80.05 (s, 6F,  $\text{CF}_3\text{SO}_3$ ), –132.84 (m, 4F, o-F), –159.46 (m, 2F, p-F), –164.60 (m, 4F, m-F). Complex **7**: Anal. Calcd. for  $\text{C}_{54}\text{H}_{36}\text{Ag}_2\text{Au}_2\text{F}_{16}\text{N}_2\text{P}_2\text{O}_6\text{S}_4$  (MW = 1888.7): C, 33.06; H, 1.92; N, 1.48; S, 6.79. Found: C, 33.27; H, 2.23; N, 1.65; S, 6.98. (LSIMS+):  $m/z = 794$  (75%,  $[\text{AgAu}(\text{SC}_6\text{F}_5)(\text{PPh}_2\text{CH}_2\text{CH}_2\text{py})]^+$ ).  $^{31}\text{P}\{^1\text{H}\}$  NMR ( $(\text{CD}_3)_2\text{CO}$ , ppm): 36.2 (s, 2P,  $\text{PPh}_2\text{CH}_2\text{CH}_2\text{py}$ ).  $^1\text{H}$  NMR ( $(\text{CD}_3)_2\text{CO}$ , ppm): 8.41 (m, 2H, py), 7.78–7.41 (m, 20 + 4H, Ph + py), 7.24 (m, 2H, py), 3.26 (m, 8H,  $\text{CH}_2$ ).  $^{19}\text{F}$  NMR ( $(\text{CD}_3)_2\text{CO}$ , ppm): –80.06 (s, 6F,  $\text{CF}_3\text{SO}_3$ ), –134.32 (m, 4F, o-F), –164.01 (m, 2F, p-F), –166.17 (m, 4F, m-F). Complex **8**: Anal. Calcd. for  $\text{C}_{46}\text{H}_{26}\text{Ag}_2\text{Au}_2\text{F}_{16}\text{N}_4\text{P}_2\text{O}_6\text{S}_4$  (MW = 1834.56): C, 30.09; H, 1.41; N, 3.05; S, 6.97. Found: C, 29.88; H, 1.30; N, 2.98; S, 6.50. MS(LSIMS+):  $m/z = 769$  (30%,

$[\text{AgAu}(\text{SC}_6\text{F}_5)(\text{PPhpy}_2)]^+$ ).  $^{31}\text{P}\{^1\text{H}\}$  NMR ( $\text{CDCl}_3$ , ppm): 30.8 (s, 2P,  $\text{PPhpy}_2$ ).  $^1\text{H}$  NMR ( $\text{CDCl}_3$ , ppm): 8.82 (m, 4H, py), 8.20 (m, 4H, py), 7.81–7.62 (m, 10 + 4H, Ph + py), 7.30 (m, 4H, py).  $^{19}\text{F}$  NMR ( $\text{CDCl}_3$ , ppm): –78.58 (s, 6F,  $\text{CF}_3\text{SO}_3$ ), –131.43 (m, 4F, o-F), –158.02 (m, 2F, p-F), –162.88 (m, 4F, m-F).

**Synthesis of  $[\text{Au}_2\text{Cu}_2(\mu\text{-SC}_6\text{F}_5)_2(\text{NCMe})_2(\mu\text{-P-N})_2](\text{PF}_6)_2$  ( $P\text{-N} = \text{PPh}_2\text{py}$  (**9**),  $\text{PPh}_2\text{CH}_2\text{CH}_2\text{py}$  (**10**), or  $\text{PPhpy}_2$  (**11**)).** To a solution of  $[\text{Au}(\text{SC}_6\text{F}_5)(\text{PPh}_2\text{py})]$  (0.066 g, 0.1 mmol),  $[\text{Au}(\text{SC}_6\text{F}_5)(\text{PPh}_2\text{CH}_2\text{CH}_2\text{py})]$  (0.068 g, 0.1 mmol), or  $[\text{Au}(\text{SC}_6\text{F}_5)(\text{PPhpy}_2)]$  (0.066 g, 0.1 mmol) in 15 mL of dichloromethane, distilled and under nitrogen atmosphere, was added  $[\text{Cu}(\text{NCMe})_4]\text{PF}_6$  (0.037 g, 0.1 mmol), and the mixture was stirred for 30 min. The solution was evaporated to 5 mL, and  $\text{Et}_2\text{O}$  was added, giving a yellow solid of **9** (0.077 g, 88%), hexane was added, giving a white solid of **10** (0.067 g, 65%), and  $\text{Et}_2\text{O}$  was added, giving a yellow solid of **11** (0.062 g, 72%). Complex **9**: Anal. Calcd. for  $\text{C}_{50}\text{H}_{40}\text{Au}_2\text{Cu}_2\text{F}_{22}\text{N}_4\text{P}_4\text{S}_2$  (MW = 1795.80): C, 33.40; H, 2.25; N, 1.56; S, 3.57. Found: C, 33.05; H, 1.98; N, 1.91; S, 3.72. MS(LSIMS+):  $m/z = 804$  (15%,  $[\text{AuCu}(\text{SC}_6\text{F}_5)(\text{PPh}_2\text{py})(\text{NCMe})_2]^+$ ),  $m/z = 723$  (100%,  $[\text{AuCu}(\text{SC}_6\text{F}_5)(\text{PPh}_2\text{py})]^+$ ).  $^{31}\text{P}\{^1\text{H}\}$  NMR ( $\text{CDCl}_3$ , ppm): 38.8.  $^1\text{H}$  NMR ( $\text{CDCl}_3$ , ppm): 8.43 (m, 2H, py), 8.01 (m, 2H, py), 7.56–7.34 (m, 20 + 4H, Ph + py), 1.97 (m, 6H,  $\text{CH}_3$ ).  $^{19}\text{F}$  NMR ( $\text{CDCl}_3$ , ppm): –74.77 (d, 12F,  $\text{PF}_6$ ,  $^1J_{\text{F-P}} = 717$  Hz), –130.48 (m, 4F, o-F), –156.04 (m, 2F, p-F), –160.20 (m, 4F, m-F). Complex **10**: Anal. Calcd. for  $\text{C}_{54}\text{H}_{48}\text{Au}_2\text{Cu}_2\text{F}_{22}\text{N}_4\text{P}_4\text{S}_2$  (MW = 1880.00): C, 34.50; H, 2.57; N, 2.98; S, 3.41. Found: C, 34.54; H, 2.16; N, 2.58; S, 3.68. MS(LSIMS+):  $m/z = 750$  (100%,  $[\text{AuCu}(\text{SC}_6\text{F}_5)(\text{PPh}_2\text{CH}_2\text{CH}_2\text{py})]^+$ ).  $^{31}\text{P}\{^1\text{H}\}$  NMR ( $(\text{CD}_3)_2\text{CO}$ , ppm): 35.3.  $^1\text{H}$  NMR ( $\text{CDCl}_3$ , ppm): 8.26 (m, 2H, py), 7.76–7.20 (m, 20 + 6H, Ph + py), 3.36 (m, 4H,  $\text{CH}_2$ ), 3.00 (m, 4H,  $\text{CH}_2$ ), 2.01 (m, 6H,  $\text{CH}_3$ ).  $^{19}\text{F}$  NMR ( $(\text{CD}_3)_2\text{CO}$ , ppm): –134.32 (m, 4F, o-F), –161.69 (m, 2F, p-F), –165.00 (m, 4F, m-F). Complex **11**: Anal. Calcd. for  $\text{C}_{48}\text{H}_{32}\text{Au}_2\text{Cu}_2\text{F}_{22}\text{N}_6\text{P}_4\text{S}_2$  (MW = 1737.72): C, 31.67; H, 1.77; N, 4.61; S, 3.52. Found: C, 31.35; H, 1.99; N, 4.06; S, 3.90. MS(LSIMS+):  $m/z = 725$  (40%,  $[\text{AuCu}(\text{SC}_6\text{F}_5)(\text{PPhpy}_2)]^+$ ).  $^{31}\text{P}\{^1\text{H}\}$  NMR ( $\text{CDCl}_3$ , ppm): 23.6.  $^1\text{H}$  NMR ( $\text{CDCl}_3$ , ppm): 8.65 (m, 4H, py), 8.37 (m, 4H, py), 8.07–7.48 (m, 10 + 8H, Ph + py), 2.01 (m, 6H,  $\text{CH}_3$ ).  $^{19}\text{F}$  NMR ( $\text{CDCl}_3$ , ppm): –74.28 (d, 12F,  $\text{PF}_6$ ,  $^1J_{\text{F-P}} = 715$  Hz), –132.78 (m, 4F, o-F), –158.93 (m, 2F, p-F), –162.81 (m, 4F, m-F).

**Synthesis of  $[\text{AgAu}_2(\mu\text{-SC}_6\text{F}_5)_2(\mu\text{-PPh}_2\text{py})_2](\text{OTf})$  (**12**).** To a solution of  $[\text{Au}(\text{SC}_6\text{F}_5)(\text{PPh}_2\text{py})]$  (0.153 g, 0.2 mmol) in 15 mL of dichloromethane was added  $\text{Ag}(\text{OTf})$  (0.025 g, 0.1 mmol). After 20 min of stirring, the solution was evaporated to 5 mL and  $\text{Et}_2\text{O}$  was added, giving a white solid of **12** (0.119 g, 76%). Anal. Calcd. for  $\text{C}_{47}\text{H}_{28}\text{AgAu}_2\text{F}_{13}\text{N}_2\text{P}_2\text{O}_3\text{S}_3$  (MW = 1575.67): C, 35.82; H, 1.79; N, 1.77; S, 6.10. Found: C, 35.63; H, 1.54; N, 1.50; S, 6.33.  $^{31}\text{P}\{^1\text{H}\}$  NMR ( $\text{CDCl}_3$ , ppm): 37.9 (s, 2P,  $\text{PPh}_2\text{py}$ ).  $^1\text{H}$  NMR ( $\text{CDCl}_3$ , ppm): 8.83 (d, 2H, py,  $^3J_{\text{H-H}} = 4.58$  Hz), 7.93 (t, 2H, py,  $^3J_{\text{H-H}} = 7.59$  Hz), 7.58–7.49 (m, 20 + 4H, Ph + py).  $^{19}\text{F}$  NMR ( $\text{CDCl}_3$ , ppm): –80.05 (s, 3F,  $\text{CF}_3\text{SO}_3$ ), –131.36 (m, 4F, o-F), –158.82 (m, 2F, p-F), –162.41 (m, 4F, m-F).

**Synthesis of  $[\text{Au}_2\text{Cu}(\mu\text{-SC}_6\text{F}_5)_2(\mu\text{-PPh}_2\text{py})_2](\text{PF}_6)$  (**13**).** To a solution of  $[\text{Au}(\text{SC}_6\text{F}_5)(\text{PPh}_2\text{py})]$  (0.153 g, 0.2 mmol) in 15 mL of dichloromethane under nitrogen atmosphere was added  $[\text{Cu}(\text{NCMe})_4]\text{PF}_6$  (0.037 g, 0.1 mmol), and the mixture was stirred for 20 min. After this time, the solution was evaporated to 5 mL and  $\text{Et}_2\text{O}$  was added, giving a yellow solid of **13** (0.107 g, 70%). Anal. Calcd. for  $\text{C}_{46}\text{H}_{28}\text{Au}_2\text{CuF}_{16}\text{N}_2\text{P}_3\text{S}_2$  (MW = 1526.5): C, 36.16; H, 1.83; N, 1.83; S, 4.19. Found: C, 35.95; H, 1.91; N, 1.71; S, 4.34. MS(LSIMS+):  $m/z = 1381$  (12%,  $[\text{Au}_2\text{Cu}(\text{SC}_6\text{F}_5)_2(\text{PPh}_2\text{py})_2]^+$ ).  $^{31}\text{P}\{^1\text{H}\}$  NMR ( $(\text{CD}_3)_2\text{CO}$ , ppm): 37.8 (s, 2P,  $\text{PPh}_2\text{py}$ ).  $^1\text{H}$  NMR ( $(\text{CD}_3)_2\text{CO}$ , ppm): 8.67 (m, 2H, py), 8.21 (m, 2H, py), 7.80 (m, 2H, py), 7.74–7.65 (m, 20 + 4H, Ph + py).  $^{19}\text{F}$  NMR ( $(\text{CD}_3)_2\text{CO}$ , ppm): –73.87 (d, 6F,  $\text{PF}_6$ ,  $^1J_{\text{F-P}} = 707$  Hz), –134.72 (m, 4F, o-F), –164.38 (m, 2F, p-F), –166.17 (m, 4F, m-F).

**Synthesis of  $[\text{Ag}_2\text{Au}_4(\mu\text{-SC}_6\text{F}_5)_3(\mu\text{-PPh}_2\text{py})_4](\text{OTf})_3$  (**14**).** To a solution of  $[\text{Au}(\text{SC}_6\text{F}_5)(\text{PPh}_2\text{py})]$  (0.263 g, 0.4 mmol) in 15 mL of dichloromethane was added  $\text{Ag}(\text{OTf})$  (0.077 g, 0.3 mmol), and the mixture was

Table 7. X-ray Data for Complexes 3, 6, 8, 11, and 15

compound	3	6 · 1/2 C <sub>6</sub> H <sub>14</sub>	8 · 2.5OEt <sub>2</sub>
formula	C <sub>22</sub> H <sub>13</sub> AuF <sub>5</sub> N <sub>2</sub> PS	C <sub>51</sub> H <sub>35</sub> Ag <sub>2</sub> Au <sub>2</sub> F <sub>16</sub> N <sub>2</sub> O <sub>6</sub> P <sub>2</sub> S <sub>4</sub>	C <sub>56</sub> H <sub>51</sub> Ag <sub>2</sub> Au <sub>2</sub> F <sub>16</sub> N <sub>4</sub> O <sub>8.5</sub> P <sub>2</sub> S <sub>4</sub>
M <sub>r</sub>	660.34	1875.66	2019.86
habit	colorless prism	pale yellow prism	yellow needle
crystal size (mm)	0.20 × 0.20 × 0.20	0.42 × 0.42 × 0.34	0.35 × 0.16 × 0.08
crystal system	triclinic	triclinic	triclinic
space group	P $\bar{1}$	P $\bar{1}$	P $\bar{1}$
cell constants:			
<i>a</i> (Å)	8.1905(16)	12.1510(19)	12.373(3)
<i>b</i> (Å)	12.172(2)	14.676(2)	12.731(3)
<i>c</i> (Å)	15.592(3)	17.507(3)	21.418(4)
α (°)	62.68(3)	97.095(2)	92.97(3)
β (°)	75.69(3)	107.186(3)	95.28(3)
γ (°)	82.13(3)	101.797(3)	95.32(3)
V (Å <sup>3</sup> )	1080.3(4)	2862.5(8)	3339.0(12)
Z	2	2	2
D <sub>x</sub> (Mg m <sup>-3</sup> )	2.030	2.176	2.009
μ (mm <sup>-1</sup> )	7.035	6.088	5.231
F(000)	628	1786	1946
T (°C)	−173	−173	−173
2θ <sub>max</sub>	50	52	50
no. of refl:			
measured	6657	16709	21757
independent	3728	10983	11474
transmissions	0.33–0.33	0.184–0.231	0.262–0.680
R <sub>int</sub>	0.010	0.019	0.036
parameters	337	752	862
restraints	0	0	158
wR(F <sup>2</sup> , all refl)	0.050	0.070	0.142
R(I > 2σ(I))	0.020	0.027	0.059
S	1.098	1.007	1.104
max Δρ (e Å <sup>-3</sup> )	2.05	1.61	4.08
compound	11	15 · H <sub>2</sub> O · 0.25CH <sub>2</sub> Cl <sub>2</sub>	
formula	C <sub>54</sub> H <sub>43</sub> Au <sub>2</sub> Cu <sub>2</sub> F <sub>22</sub> N <sub>9</sub> P <sub>4</sub> S <sub>2</sub>	C <sub>86</sub> H <sub>56</sub> Au <sub>4</sub> Cu <sub>2</sub> F <sub>33</sub> N <sub>4</sub> P <sub>7</sub> S <sub>3</sub> · H <sub>2</sub> O · 0.25CH <sub>2</sub> Cl <sub>2</sub>	
M <sub>r</sub>	1944.99	3039.51	
habit	yellow prism	yellow tiny block	
crystal size (mm)	0.20 × 0.17 × 0.12	0.04 × 0.02 × 0.01	
crystal system	triclinic	monoclinic	
space group	P $\bar{1}$	P2 <sub>1</sub> /c	
cell constants:			
<i>a</i> (Å)	11.214(2)	20.373(5)	
<i>b</i> (Å)	15.520(3)	14.817(4)	
<i>c</i> (Å)	18.755(4)	32.056(8)	
α (°)	95.95(3)	90.0	
β (°)	92.64(3)	97.785(5)	
γ (°)	106.43(3)	90.0	
V (Å <sup>3</sup> )	3104.1(11)	9588(4)	
Z	2	4	
D <sub>x</sub> (Mg m <sup>-3</sup> )	2.081	2.106	
μ (mm <sup>-1</sup> )	5.671	6.288	
F(000)	1872	5778	
T (°C)	−173	−123	
2θ <sub>max</sub>	50	54	

Table 7. Continued

compound	11	15 · H <sub>2</sub> O · 0.25CH <sub>2</sub> Cl <sub>2</sub>
no. of refl:		
measured	19972	60656
independent	10868	22765
transmissions	0.396–0.549	0.787–0.940
R <sub>int</sub>	0.015	0.085
parameters	858	1081
restraints	0	126
wR(F <sup>2</sup> , all refl)	0.069	0.211
R(I > 2σ(I))	0.030	0.092
S	1.074	1.106
max Δρ (e Å <sup>-3</sup> )	1.80	2.68

stirred for 20 min. The AgCl that formed was filtered through Celite, and the solution was evaporated to 5 mL. Et<sub>2</sub>O was added giving a white solid of **14** (0.259 g, 76%). <sup>31</sup>P{<sup>1</sup>H} NMR (CDCl<sub>3</sub>, ppm): 38.9 (s, 4P, PPh<sub>2</sub>py). <sup>1</sup>H NMR (CDCl<sub>3</sub>, ppm): 8.89 (d, 4H, py, <sup>3</sup>J<sub>H-H</sub> = 4.7 Hz), 7.95 (m, 4H, py), 7.60–7.54 (m, 40 + 4H, Ph + py), 7.37 (m, 4H, py). <sup>19</sup>F NMR (CDCl<sub>3</sub>, ppm): –80.05 (s, 3F, CF<sub>3</sub>SO<sub>3</sub>), –135 (m, 6F, o-F), –157.94 (m, 3F, p-F), –162.25 (m, 6F, m-F).

**Synthesis of [Au<sub>4</sub>Cu<sub>2</sub>(μ-SC<sub>6</sub>F<sub>5</sub>)<sub>3</sub>(μ-PPh<sub>2</sub>py)<sub>4</sub>](PF<sub>6</sub>)<sub>3</sub> (**15**).** To a solution of [Au(SC<sub>6</sub>F<sub>5</sub>)(PPh<sub>2</sub>py)] (0.263 g, 0.4 mmol) in 15 mL of dichloromethane under nitrogen atmosphere was added [Cu(NCMe)<sub>4</sub>]-PF<sub>6</sub> (0.111 g, 0.3 mmol). After stirring for 30 min, the mixture was filtered through Celite. The solution was concentrated to 5 mL, and addition of Et<sub>2</sub>O gave a yellow solid of **15** (0.280 g, 86%). Anal. Calcd. for C<sub>86</sub>H<sub>56</sub>Au<sub>4</sub>Cu<sub>2</sub>F<sub>33</sub>N<sub>4</sub>P<sub>7</sub>S<sub>3</sub> (MW = 3000.31): C, 34.42; H, 1.88; N, 1.86; S, 3.20. Found: C, 34.61; H, 1.81; N, 1.69; S, 3.44. <sup>31</sup>P{<sup>1</sup>H} NMR ((CD<sub>3</sub>)<sub>2</sub>CO, ppm): 37.6 (s, 4P, PPh<sub>2</sub>py). <sup>1</sup>H NMR ((CD<sub>3</sub>)<sub>2</sub>CO, ppm): 8.71 (m, 4H, py), 8.22 (m, 4H, py), 7.83 (m, 4H, py), 7.74–7.75 (m, 40 + 4H, Ph + py). <sup>19</sup>F NMR (CDCl<sub>3</sub>, ppm): 73.00 (d, 18F, PF<sub>6</sub>, <sup>1</sup>J<sub>F-P</sub> = 714 Hz), –130.50 (m, 1F, o-F), –131.66 (m, 3F, o-F), –132.41 (m, 1F, o-F), –132.91 (m, 1F, o-F), –162.62 (m, 2F, p-F), –156.21 (m, 1F, p-F), –160.20 (m, 1F, m-F), –160.85 (m, 1F, m-F), –161.38 (m, 1F, m-F), –161.86 (m, 3F, m-F).

**Crystallography.** Crystals were mounted in inert oil on glass fibers and transferred to the cold gas stream of a Smart Apex CCD (**6**) or Xcalibur Oxford Diffraction (**3**, **8**, **11**) diffractometer equipped with a low-temperature attachment. Data were collected using monochromated Mo Kα radiation (λ = 0.71073 Å), scan type ω. In the case of **15**, data were obtained at 150(1) K from a BrukerAXS SMART APEXII CCD diffractometer installed at station 9.8 of the SRS Daresbury Laboratory. Synchrotron radiation was monochromated with a silicon (111) crystal (λ = 0.68940 Å); data were collected using narrow frames (0.3° in ω). In all cases, cell parameters were refined from the observed setting angles and detector positions of a set of strong reflections, and instrument and crystal stability were evaluated during data collection from measurement of equivalent reflections at different measuring times; no important variations were observed. Data were corrected for Lorentz and polarization effects, and a semiempirical absorption correction (SADABS),<sup>24</sup> based on repeated and symmetry-equivalent reflections, was also applied.

The structures were solved by direct methods and refined on F<sup>2</sup> using the program SHELXL-97.<sup>25</sup> All non-hydrogen atoms were refined anisotropically. In the case of **15**, several situations of static disorder were detected affecting phenyl rings of the PPh<sub>2</sub>py ligands and some of the PF<sub>6</sub> anions. Two solvent molecules (H<sub>2</sub>O and CH<sub>2</sub>Cl<sub>2</sub>) were also observed in the crystal structure of **15**. In all cases, hydrogen atoms were included in calculated positions and refined using a riding model. Refinements were carried out by full-matrix least-squares on F<sup>2</sup> for all data. Further details of the data collection and refinement are given in Table 7.

## ASSOCIATED CONTENT

**Supporting Information.** Five X-ray crystallographic files, in CIF format, for compounds **3**, **6**, **8**, **11**, and **15**. This material is available free of charge via the Internet at <http://pubs.acs.org>.

## AUTHOR INFORMATION

### Corresponding Author

\*E-mail: [gimeno@unizar.es](mailto:gimeno@unizar.es).

## ACKNOWLEDGMENT

Authors thank CCLRC Daresbury Laboratory for allocation of synchrotron beam time (AP42) and the Ministerio de Ciencia e Innovación (CTQ2010-20500-C02-01) and (MICINN/FEDER, CSD2006-0015) for financial support.

## REFERENCES

- (1) (a) *Modern Supramolecular Gold Chemistry: Gold–Metal Interactions and Applications*; Laguna, A., Ed.; Wiley-VCH: New York, 2008. (b) Yue, C.; Yan, C.; Feng, R.; Rui, W.; Wu, M.; Chen, L.; Jiang, F.; Hong, M. *Inorg. Chem.* **2009**, *48*, 2873. (c) Barbieri, A.; Accorsi, G.; Armaroli, N. *Chem. Commun.* **2008**, 2185. (d) Teets, T. S.; Partyka, D. V.; Esswein, A. J.; Updegraff, J. B., III; Zeller, M.; Hunter, A. D.; Gray, T. G. *Inorg. Chem.* **2007**, *46*, 6218. (e) Liu, B.; Yuan, Q. *Inorg. Chem.* **2005**, *8*, 1022. (f) Che, C.-M.; Lai, S.-W. *Coord. Chem. Rev.* **2005**, *8*, 1022. (g) Chui, S. S. Y.; Ng, M. F. Y.; Che, C.-M. *Chem.—Eur. J.* **2005**, *11*, 1739. (h) Yam, V. W.-W.; Cheung, K.-L.; Cheng, E. C.-C.; Zhu, N.; Cheung, K.-K. *Dalton Trans.* **2003**, 1830. (i) Ford, P. C.; Canati, E.; Bourassa, J. *Coord. Chem. Rev.* **1999**, *99*, 3625. (j) Yam, V. W.-W.; Lo, K. K.-W. *Chem. Soc. Rev.* **1999**, *28*, 323. (k) Fernandez, E. J.; Laguna, A.; López-de-Luzuriaga, J. M.; Monge, M.; Rodríguez-Castrillo, M. *Open Inorg. Chem. J.* **2008**, *2*, 73. (l) Yam, V. W.-W.; Lo, K. K.-W.; Fung, W. K.-M.; Wang, C.-R. *Coord. Chem. Rev.* **1998**, *171*, 17.
- (2) (a) Schmidbaur, H.; Cronje, S.; Djorjevic, B.; Schuster, O. *Chem. Phys.* **2005**, *311*, 151. (b) Pyykkö, P. *Chem. Rev.* **1997**, *97*, 597. (c) Pyykkö, P. *Chem. Soc. Rev.* **2008**, *37*, 1967.
- (3) (a) Forward, J. M.; Fackler, J. P., Jr.; Assefa, Z. *Optoelectronic Properties of Inorganic Compounds*; Roundhill, D. M., Fackler, J. P., Jr., Eds.; Plenum Press: New York, 1999; p 195. (b) Balch, A. L. *Gold Bull.* **2004**, *37*, 1. (c) Yam, V. W.-W.; Chan, C. L.; Li, C. K.; Wong, K. M. C. *Coord. Chem. Rev.* **2001**, *216–217*, 173. (d) Yam, V. W.-W. *Chem. Soc. Rev.* **2008**, *37*, 1806. (e) Yam, V. W.-W.; Tao, C. H. In *Gold*; Corti, C., Holliday, R., Eds.; CRC Press: Boca Raton, FL, 2010; p 69. (f) Che, C. M.; Lai, S. W. In *Gold Chemistry*; Mohr, F., Ed.; Wiley-VCH: Weinheim, Germany, 2009; p 249. (g) Balch, A. L. *Struct. Bonding (Berlin, Ger.)* **2007**, *123*, 1. (h) Abdou, H.; Mohamed, A. A.; Fackler, J. P.,

Jr. *J. Cluster Sci.* **2007**, *18*, 630. (i) Manbeck, G. F.; Brennessel, W. W.; Stockland, R. A., Jr.; Eisenberg, R. *J. Am. Chem. Soc.* **2010**, *132*, 12307.

(4) (a) Wang, Q. M.; Lee, Y. A.; Crespo, O.; Deaton, J.; Tang, C.; Gysling, H. J.; Gimeno, M. C.; Larraz, C.; Villacampa, M. D.; Laguna, A.; Eisenberg, R. *J. Am. Chem. Soc.* **2004**, *126*, 9488. (b) Crespo, O.; Gimeno, M. C.; Laguna, A.; Larraz, C.; Villacampa, M. D. *Chem.—Eur. J.* **2007**, *13*, 235.

(5) (a) Yam, V. W. W.; Cheng, E. C. C.; Cheung, K. K. *Angew. Chem., Int. Ed.* **1999**, *38*, 197. (b) Yam, V. W. W.; Cheng, E. C. C.; Zhou, Z. Y. *Angew. Chem., Int. Ed.* **2000**, *39*, 1683. (c) Yam, V. W. W.; Cheng, E. C. C.; Zhu, N. *Angew. Chem., Int. Ed.* **2001**, *40*, 1763.

(6) Gimeno, M. C.; Laguna, A. *Comprehensive Coordination Chemistry II*; McCleverty, J. A., Meyer, T. J., Eds.; Elsevier: New York, 2003; Vol 5, p 911.

(7) (a) Gimeno, M. C. *Handbook of Chalcogen Chemistry: New Perspectives in Sulfur, Selenium and Tellurium*; Devillanova, F. A., Ed.; The Royal Society of Chemistry: Cambridge, U.K., 2007; p 33. (b) Dell'Amico, D. B.; Calderazzo, F.; Pasqualetti, N.; Hubener, R.; Maichle-Mossmar, C.; Strahle, J. *J. Chem. Soc., Dalton Trans.* **1995**, 3917. (c) Sladek, A.; Angermaier, K.; Schmidbaur, H. *Chem. Commun.* **1996**, 1959. (d) Barranco, E. M.; Gimeno, M. C.; Laguna, A.; Villacampa, M. D.; Jones, P. G. *Inorg. Chem.* **1999**, *38*, 702.

(8) Daniel, M. C.; Astruc, D. *Chem. Rev.* **2004**, *104*, 293.

(9) Toyota, A.; Yamaguchi, T.; Igashira-Kamiyama, A.; Kawamoto, T.; Konno, T. *Angew. Chem., Int. Ed.* **2005**, *44*, 1088.

(10) Hao, L.; Mansour, M. A.; Lachicotte, R. J.; Gysling, H. J.; Eisenberg, R. *Inorg. Chem.* **2000**, *39*, 5520.

(11) Nunokawa, K.; Onaka, S.; Mizuno, Y.; Okazaki, K.; Sunahara, T.; Ito, M.; Yaguchi, M.; Imai, H.; Inoue, K.; Ozeki, T.; Chiba, H.; Yosida, T. *J. Organomet. Chem.* **2005**, *690*, 48.

(12) Crespo, O.; Canales, F.; Gimeno, M. C.; Jones, P. G.; Laguna, A. *Organometallics* **1999**, *18*, 3142.

(13) Watase, S.; Kitamura, T.; Kanehisa, N.; Shizuma, M.; Nakamoto, M.; Kai, Y.; Yanagida, S. *Chem. Lett.* **2003**, *32*, 1070.

(14) (a) Canales, F.; Gimeno, M. C.; Laguna, A.; Villacampa, M. D. *Inorg. Chim. Acta* **1996**, *244*, 95. (b) Canales, S.; Crespo, O.; Gimeno, M. C.; Jones, P. G.; Laguna, A.; Mendizábal, F. *Organometallics* **2000**, *19*, 4985.

(15) (a) Forward, J. M.; Bohmann, D.; Fackler, J. P., Jr.; Staples, R. J. *Inorg. Chem.* **1995**, *34*, 6330. (b) Tzeng, B.-C.; Chan, C.-K.; Cheung, K.-K.; Che, C. M.; Peng, S. M. *Chem. Commun.* **1997**, 135. (c) Tzeng, B. C.; Yeh, H. T.; Huang, Y. C.; Chao, H. Y.; Lee, G. H.; Peng, S. M. *Inorg. Chem.* **2003**, *42*, 6008. (d) Chen, Z. N.; Zhao, N.; Fan, Y.; Ni, J. *Coord. Chem. Rev.* **2009**, *253*, 1. (e) Tiekink, E. R. T.; Kang, J.-G. *Coord. Chem. Rev.* **2009**, *253*, 1627.

(16) Zhang, T.; Chen, C.; Qin, Y.; Meng, X. *Inorg. Chem. Commun.* **2006**, *9*, 72.

(17) Calhorda, M. J.; Ceamanos, C.; Crespo, O.; Gimeno, M. C.; Laguna, A.; Larraz, C.; Vaz, P. D.; Villacampa, M. D. *Inorg. Chem.* **2010**, *49*, 8255.

(18) DATAMAX 2.20; Jobin Yvon, Inc.: Edison, NJ, 2001.

(19) *Origin 5.0*; Microcal Software, Inc.: Northampton, MA, 1991.

(20) Casares, J. A.; Espinet, P.; Soulantica, K.; Pascual, I.; Orpen, A. G. *Inorg. Chem.* **1997**, *36*, 5251.

(21) Xie, Y.; Chung, L. L.; Yang, Y.; Retting, S. J.; James, B. R. *Can. J. Chem.* **1992**, *70*, 751.

(22) (a) Ang, H. G.; Know, W. E.; Mok, K. F. *Inorg. Nucl. Chem. Lett.* **1972**, *8*, 829. (b) Inoguchi, Y.; Milewski-Mahrla, B.; Schmidbaur, H. *Chem. Ber.* **1982**, *115*, 3085. (c) Alcock, N. W.; Moore, P.; Lampe, P. A.; Mok, K. F. *J. Chem. Soc., Dalton Trans.* **1982**, 207.

(23) Kubas, G. J. *Inorg. Synth.* **1979**, *19*, 90.

(24) Sheldrick, G. M. *SADABS, Program for Corrections of Area Detector Data*; University of Göttingen: Göttingen, Germany, 1999.

(25) Sheldrick, G. M. *SHELXL-97, A Program for Crystal Structure Refinement*; University of Göttingen: Göttingen, Germany, 1997.

$[\text{Au}_{12}(\mu_3\text{-S})_4(\mu\text{-dppm})_6](\text{PF}_6)_4$  in the introduction and for compounds 14 and 15 in the Experimental Section. This information is corrected in this new version published on August 26, 2011.

## NOTE ADDED AFTER ASAP PUBLICATION

An earlier version of this paper published on the web on August 23, 2011 contained errors in the chemical formulas for